Iterative Receiver in Multiuser Relaying Systems with Fast Frequency-Hopping Modulation

A Thesis Submitted
to the College of Graduate Studies and Research
in Partial Fulfillment of the Requirements
for the Degree of Master of Science
in the Department of Electrical and Computer Engineering
University of Saskatchewan

by

Tung T. Nguyen

Saskatoon, Saskatchewan, Canada

Permission to Use

In presenting this thesis in partial fulfillment of the requirements for a Postgraduate degree from the University of Saskatchewan, it is agreed that the Libraries of this University may make it freely available for inspection. Permission for copying of this thesis in any manner, in whole or in part, for scholarly purposes may be granted by the professors who supervised this thesis work or, in their absence, by the Head of the Department of Electrical and Computer Engineering or the Dean of the College of Graduate Studies and Research at the University of Saskatchewan. Any copying, publication, or use of this thesis, or parts thereof, for financial gain without the written permission of the author is strictly prohibited. Proper recognition shall be given to the author and to the University of Saskatchewan in any scholarly use which may be made of any material in this thesis.

Request for permission to copy or to make any other use of material in this thesis in whole or in part should be addressed to:

Head of the Department of Electrical and Computer Engineering
57 Campus Drive
University of Saskatchewan
Saskatoon, Saskatchewan, Canada
S7N 5A9

Acknowledgments

I would like to express my deepest appreciation and gratitude to my supervisor, Professor Ha Nguyen for his great intellectual support during my studies. With his vast knowledge and skills, he has helped me go through difficulties with constant encouragement and influential discussions. His thoughtful advice often served to give me a sense of direction during my M.Sc. studies. For those reasons, I am deeply grateful for his valuable guidance and directives.

My special thanks goes to Professor Eric Salt who taught me many exciting courses. I admire his bright wisdom and his distinguished character, whose thoughtful instructions often go well with a great sense of humor. Without him, I would not be able to enjoy learning that much.

I would also like to thank my family for the endless support they provided through my entire life and in particular, I must acknowledge my wife and my brother, without whose love, encouragement and sacrifice, I would not have finished this thesis.

Abstract

In this thesis, a novel iterative receiver and its improved version are proposed for relay-assisted multiuser communications, in which multiple users transmit to a destination with the help of a relay and using fast frequency-hopping modulation. Each user employs a channel encoder to protect its information and facilitate interference cancellation at the receiver. The signal received at the relay is either amplified, or partially decoded with a simple energy detector, before being forwarded to the destination. Under flat Rayleigh fading channels, the receiver at the destination can be implemented non-coherently, i.e., it does not require the instantaneous channel information to demodulate the users' transmitted signals. The proposed iterative algorithm at the destination exploits the soft outputs of the channel decoders to successively extract the maximum likelihood symbols of the users and perform interference cancellation. The iterative method is successfully applied for both cases of amplify-and-forward and partial decode-and-forward relaying. The error performance of the proposed iterative receiver is investigated by computer simulation. Under the same spectral efficiency, simulation results demonstrate the excellent performance of the proposed receiver when compared to the performance of decoding without interference cancellation as well as the performance of the maximum likelihood multiuser detection previously developed for uncoded transmission. Simulation results also suggest that a proper selection of channel coding schemes can help to support significant more users without consuming extra system resources.

In addition, to further enhance the receiver's performance in terms of the bit error rate, an improved version of the iterative receiver is presented. Such an improved receiver invokes inner-loop iterations between the channel decoders and the demappers in such a way that the soft outputs of the channel decoders are also used to refine the outputs of the demappers for every outer-loop iteration. Simulation results indicate a performance gain of about 2.5dB by using the two-loop receiver when compared to the performance of the first proposed receiver.

Table of Contents

List of Figures

List of Abbreviations

M-FSK	M-ary Frequency Shift Keying
AF	Amplify-and-Forward
BER	Bit Error Rate
CDMA	Code Division Multiple Access
DF	Decode-and-Forward
DPSK	Differential Phase-Shift Keying
FDMA	Frequency-Division Multiple Access
FEC	Forward Error Correction
FFH	Fast Frequency Hopping
FH	Frequency Hopping
FHMA	Frequency Hopping Multiple Access
GSM	Global System for Mobile Communications
IIC	Iterative Interference Cancellation
LDPC	Low-Density Parity-Check
MA	Multiple-Access
MAI	Multiple Access Interference
MAP	Maximum A Posteriori Probability
ML	Maximum Likelihood
ML-MUD	Maximum-Likelihood Multiuser Detector

MUI	Multiuser Interference
PDAF	Partial Decode-and-Forward
SFH	Slow Frequency Hopping
SIC	Soft Interference Cancellation
SISO	Soft Input Soft Output
TDMA	Time-Division Multiple Access
TF	Time-Frequency

1. Introduction

Wireless communication networks are being considered as the fastest growing segment of the communication industry [1]. Before becoming one of the most crucial technologies for everyday life, it had a long history of development [2]. In 1865, Maxwell published his theoretical work on describing the movement of electromagnetic waves through space, which set a milestone in radio communication. Before the publication of Maxwell's work, people had no idea about the existence of "waves" that cannot be seen by bare eyes. Maxwell, by the way, had never seen a radio and had no actual experience with radio waves himself. But his theories paved the way for the next set of crucial inventions. First, an experiment which marked the birth of radio transmission was performed in 1897, when Marconi sent a radio telegraph across the English Channel [3]. The public use of radio began in 1907 and there have been so many great contributions since then, including the works of Armstrong (who invented wide-band frequency modulation), De Forest (who created the amplifying vacuum tubes) and Viterbi (who came up with digital decoding and code-division multiple access (CDMA) technique) and so many more that are not possible to list here. Now there are more people working in wireless communication industry than at any other time in history [4]. Wireless communication systems have experienced exponential growth over the last decades and there are currently more than six billion subscribers worldwide [5].

While having the ability to send information over the air, wireless communication systems often suffer from channel attenuations due to propagation path loss, shadowing loss and absorption loss. Furthermore, a signal transmitted through a wireless channel typically experiences random variations due to the presence of objects in the signal path, giving rise to random variations of the received power at the destination. Such random variations are

generally referred to as fading effect which varies in time and depends on the geographical positions of transmitters and receivers. To maintain the quality of data services under such fading environment, one can increase the transmit power, employ a wider transmission bandwidth or use multi-input multi-output communications [6]. However, due to size, cost, and/or hardware limitations, a wireless device may not be able to support such multiple-antenna implementation. For those reasons, relay-assisted transmission has emerged as one of the promising solutions to deal with the fading problem.

A relay is a system that receives and retransmits the signal among stations or between base stations and mobile devices. By doing so, a relay can help increasing the throughput and/or extending the coverage of a wireless communication system. The infrastructure of wireless relays does not need any wired connection and it can be installed at either a fixed station or a mobile vehicle. Furthermore, a relay's structure is often less complex and consumes less power than a base station. Relay transmission, therefore, offers overall cost saving when being used in a wireless communication system. As a matter of fact, during the 1950s, AT&T had established a long-distance wireless link between New York and Boston using relays [7]. The main reason was that a direct communication link would not be possible due to the curvature of the earth and natural obstacles. A few decades later, people witnessed the success of satellite communications [8]. In such an application, a satellite plays the role of a relay and was often refereed to as a "mirror" or "repeater" in outer space. A satellite receives message signals from a sender and may forward the messages to some other satellites so that the messages can be transmitted back to the earth. Being considered the only truly commercial space technology, generating billions of dollars annually in sales of products and services, satellite communication has motivated the theoretical study of relay systems in early 1970s. Since then, deploying relays has become essential in any long distance communication systems.

Influenced by the rapid development of wireless radios, personal communication devices are being made smaller and become more accessible to majority of human population. Consequently, communication networks are becoming larger with the capability of serving multiple devices at the same time. It is common that two or more geographically separated nodes

attempt to exchange binary data simultaneously [9]. This scenario is generally known as a multiple-access (MA) communication system, which was originally studied by Liao [10] in 1972 and has been followed by many researchers [11–13]. It is pointed out that using channel coding is essential for multiple access channels [13] as it provides crucial information protection. Moreover, using channel coding makes the output signals (from multiple transmitters) uncorrelated. This is beneficial since it has been shown that the capacity of a multiple access channel, which is equal to the mutual information between the input and output of the channel, is maximized when all the transmitted signals are statistically independent [10]. Early investigation on code construction for MA channels focuses mainly on block coding [14–16] and the maximum achievable capacity was analyzed. However, block-coded MA systems require different constituent codes at the transmitters, thus introducing extra complexity to both the transmitting and receiving sides. Fortunately, inspired by the success of turbo codes [17, 18], a simple, yet effective approach for coding in a MA system was found with the introduction of interleaving and iterative processing. Interleaving is a low-complexity operation that often takes place after forward error correction (FEC) coding. The possibility of employing interleaving for user separation has been widely investigated in [19–21]. Furthermore, the ability to approach the capacity of a MA channel has been demonstrated for systems using interleaving [22, 23].

This thesis is concerned with an MA wireless communication system, in which multiple users wish to reliably deliver their information to a receiver with the help of a relay. The model is shown in Fig. 1.1. Since the relay operates in a half-duplex mode, i.e., it cannot transmit and receive at the same time, communication between sources and destination is carried out in two time slots. In the first time slot, the relay receives signals transmitted simultaneously from all users. It then processes and forwards the result to the destination in the second time slot. Also note that during the first time slot, signal from one user should not severely interfere with signals from other users. This can be done by using an appropriate channel access method. For example, signals from multiple users can be separated in the time domain (by using time-division multiple access (TDMA)), frequency domain (by using frequency-division multiple access (FDMA)) or code domain (by using code-division multiple

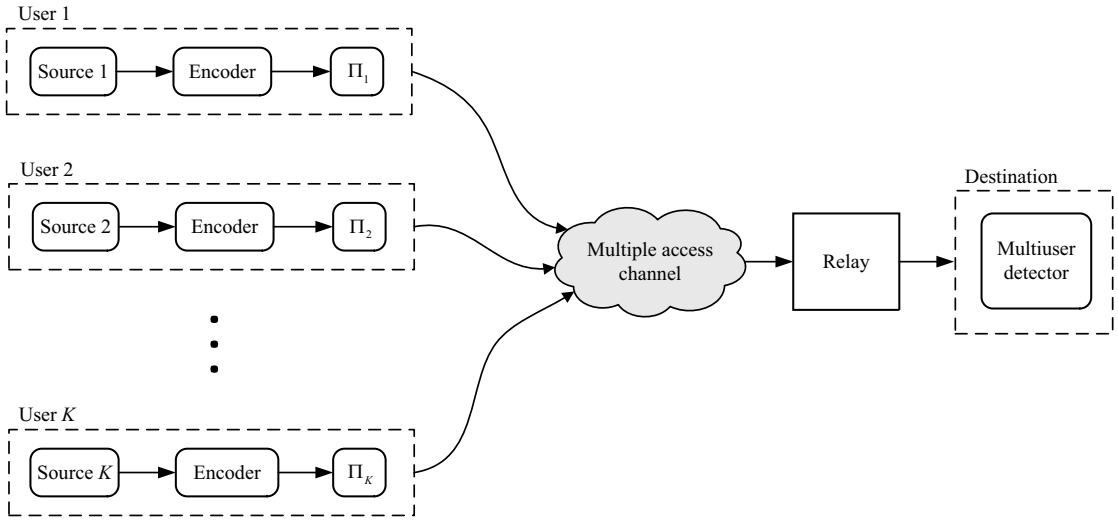

Figure 1.1 Multi-user one-way relaying system.

access (CDMA)).

When fast frequency hopping (FFH) [24] is selected as the modulation technique, multi-user signals can only be made semi-orthogonal in both frequency and time domains. However, by using FFH modulation for all transmission links, the system can benefit from:

- **Frequency diversity**: By dividing the system's bandwidth into many sub-bands, the main advantage of FFH modulation is that it is highly tolerant of narrow-band interference. The FFH modulation, therefore, can also effectively mitigate the inherent fading effects of wireless transmission. With high frequency diversity order, the FFH system can co-operate with other systems employing different modulation types by sharing the same frequency band.

- **Time diversity**: One FFH symbol is spread to multiple hops in different time slots. The hopping is considered non-coherently related, thus making the FFH system resistant to burst noise.

- **Non-coherent detection**: Owing to the fact that FFH signals can be detected non-coherently, the impacts of phase distortion and frequency offset are minimized with

this modulation method. Also, without requiring the channel state information (CSI), the receiver's structure can be simplified.

For the system in Fig. 1.1, the main source of performance degradation comes from multiple access interference (MAI) in the first time slot, which also propagates to the destination in the second time slot. MAI, also known as multiuser interference (MUI) arises because signals from multi-users are not completely orthogonal, which is an inherent issue of FFH modulation. The system performance therefore depends on how well the receiver can distinguish one's transmitted signal from the others. For the past few decades, there were significant research studies on multi-user detection (MUD). While it is commonly known that the maximum-likelihood (ML) joint multi-user detection gives the best performance, its excessively high computational complexity makes it very expensive (in terms of hardware cost), if not impossible, for practical implementation [25]. This difficulty motivates the iterative processing approach, which was introduced shortly after the discovery of turbo codes. In contrast to the classical approach, where demodulating and decoding are performed separately one after another, an iterative receiver exchanges probabilistic quantities among its modules and gradually approaches the optimum detection bound [26]. Specifically, the iterative processing principle allows earlier stages (e.g., the demodulator) to refine their processing based on information obtained from later stages (e.g., channel decoder). While most contributions on iterative receivers focus on CDMA and point-to-point communications, no iterative multi-user receiver for FFH modulated system has been developed for wireless relay networks. Developing an iterative receiver at the destination node for the system in Fig. 1.1 is precisely the main objective of this thesis.

The remainder of this chapter gives an overview of the thesis' contributions and its organization.

In Chapter 2, a background of multi-user one-way relay systems considered in this thesis is provided. Different scenarios of relay communications are discussed. In addition, the advantages and disadvantages of different signal processing methods, including amplify-and-forward, decode-and-forward as well as partial decode-and-forward are explained. The

purpose is to give a general introduction to systems investigated in the literature that are related to the work in this thesis. Relevant to the iterative receiver proposed in this thesis, the technique of FFH modulation with non-coherent detection are also described in this chapter. Conventional algorithms to detect FFH signals will also be presented.

Chapter 3 starts with an introduction of the multi-user relay system under consideration. To facilitate the transmission from sources to a destination via a relay, two relaying schemes are presented. The first scheme is the well-known amplify-and-forward relaying, while the second scheme is a threshold-based partial decode-and-forward relaying, which is specifically designed for FFH modulation. Depending on the signal processing scheme employed at the relay, the receiver at the destination needs to detect the information transmitted by multiple users. Exploiting the unique pattern of the signal from each user, a method to jointly detect multiple users' signals is developed. The proposed detection algorithm relies on the soft interference cancellation (SIC) that incorporates feedback information from the decoders. For both relaying schemes mentioned above, the performance of the proposed receiver shows a remarkable improvement over the conventional uncoded system under the same spectral efficiency. In addition, while the partial decode-and-forward relaying scheme requires extra complexity at the relay, its corresponding receiver at the destination is simpler but yields better performance than the amplify-and-forward relaying scheme.

Chapter 4 presents an important improvement to the receiver designed in Chapter 3. Specifically, by introducing a soft demapper between the SIC module and the channel decoder, the iterative process is expanded so that probabilistic soft information is exchanged among three modules: the interference canceller, the soft demapper and the channel decoder. The receiver is designed to incorporate an inner iterative process between the soft demapper and the channel decoder to further refine the outcome of the multi-user detector. This in effect introduces two-loop operation: The outer-loop processing is where the soft information is exchanged between the SIC and the channel decoder, whereas for the inner-loop processing the extrinsic information is passed between the soft demapper and the channel decoder. Simulation results are also provided in this chapter to demonstrate performance superiority of the improved receiver.

Finally, Chapter 5 draws conclusions and offers suggestions for further studies.

2. Background

2.1 Relay Communications

In conventional wireless communication systems, data transmission occurs directly between the transmitter and the receiver. This scenario is commonly known as single-hop communication, as shown in Fig. 2.1-(a). A mobile terminal (user node) tries to communicate with a base station (destination node) without any help of intermediate devices. However, a user node could be located outside the service area of the destination or located in an unfavorable location resulting in coverage dead spots. For example, a user node could be surrounded by large buildings or located in a valley shadowed by mountains. Such situations elevate the effect of path-loss, which is caused by the reduction of power density of an electromagnetic wave as it propagates through space. As such, the demand for constant data service requires appropriate techniques to combat signal attenuations in such situations.

Relaying or two-hop communication is a practical solution for extending the coverage area in a cost effective way. Relaying implies that the original transmitted signal passes through one or more intermediate nodes before reaching the destination. As illustrated in Fig. 2.1-(b), a relay splits a longer communication path into shorter ones, therefore providing the ability to reduce overall path-loss. Moreover, by employing a relay, source-destination communication link can be re-routed around obstacles to overcome shadowing loss, as seen in Fig. 2.2. Typically, relaying is considered as an add-on to traditional point-to-point wireless systems, whose main goal is to boost the system's performance under severe signal attenuations.

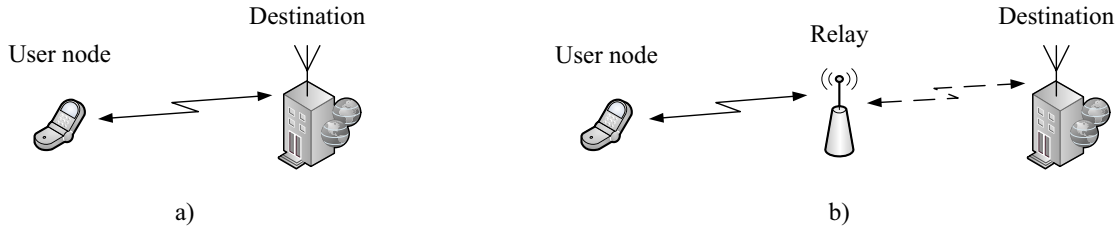

Figure 2.1 Wireless communications: (a) Single-hop direct transmission, and (b) Two-hop relay transmission.

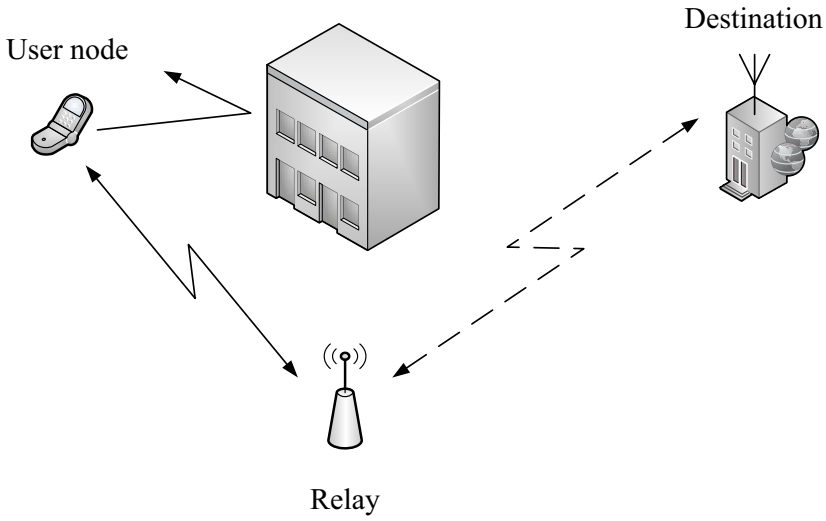

Figure 2.2 Overcome shadowing by employing a relay.

2.1.1 Relaying Topologies

Different relaying topologies have been proposed so that single/multiple relay(s) can effectively help single/multiple source(s) to communicate with single/multiple destination(s). In this section, two variants of relaying topologies are presented, which are one-way relaying and multi-way relaying.

One-Way Relaying

The most basic relying setup, as illustrated in Fig. 2.1-(b), consists of a single user and a single destination, with one relay in between to reduce the distance of one-hop communication. As the relay operates in a half-duplex mode, the source sends its data to the relay

in the first phase (marked by solid arrow) and the relay forwards its received signal to the destination in the second phase (marked by dashed arrow). It is pointed out that spatial diversity may be achieved by also utilizing the direct-link transmission [27], i.e., when the destination also takes into account the weak signal from the source in the first phase and combines it with the relayed signal in the second phase. Furthermore, spatial diversity can be enhanced by introducing more relays to the system [28], as shown in Fig. 2.3-(a). Here multiple relays help one source to communicate with the destination. With this setup, the relays are geographically separated and operate like a virtual antenna array. This setup can combat severe multipath fading by creating multiple independent communication paths between the source and the destination. However, it is very inefficient to deploy many relays just to support a single source-destination transmission. On the other hand, a much more efficient topology is to use a single relay to help multiple users. This topology is illustrated in Fig. 2.3-(b), in which all the source nodes simultaneously communicate with the single relay in the first phase and the relay communicates with the destination in the second phase. As pointed out before, ideally, signals from the multiple sources should be made orthogonal or semi-orthogonal to avoid or minimize multiple-access interference.

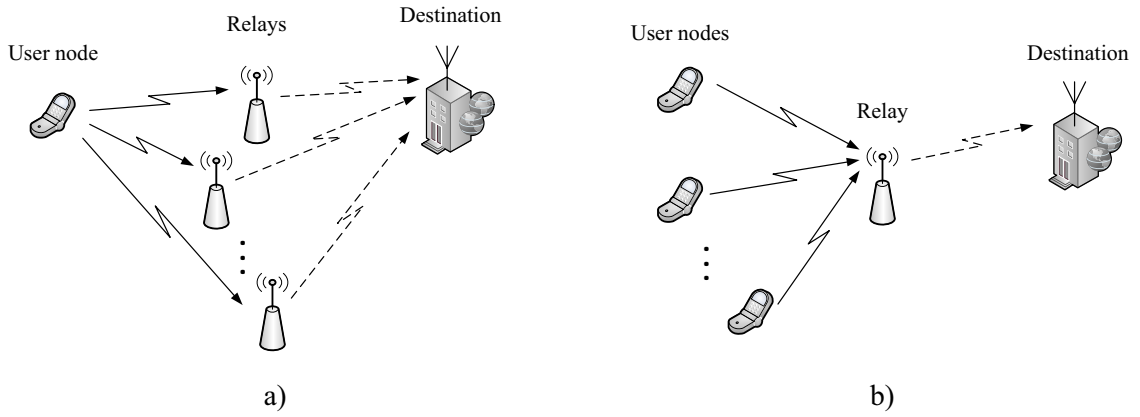

Figure 2.3 One-way relaying: (a) Multiple relays help one user; (b) Single relay helps multiple users.

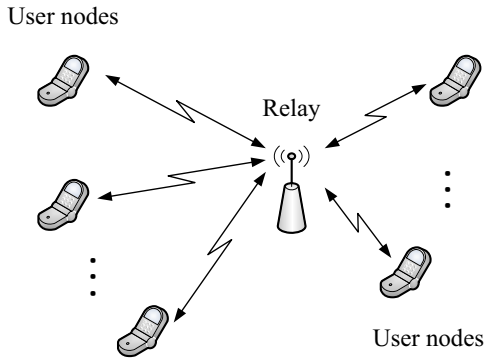

Figure 2.4 Multi-way relaying.

Multi-Way Relaying

Fig. 2.4 illustrates another relaying topology, in which multiple users exchange their messages with the help of a single relay. Such information exchange can also be carried out in two time slots. Communication in the first time slot, which is also referred to as multiple-access phase [29], is similar to that of one-way relaying, where all users simultaneously send signals to the relay. Then the relay processes received signals (e.g., amplify, decode, compress or functional decode [30]) before broadcasting a new signal back to all users in the second phase. The signal transmitted by the relay in the second phase includes messages from all the users. Since each user already knows its own message, it can subtract out its own information before decoding other users' messages more efficiently [31].

2.1.2 Relay Classification

A relay processes the received signal before sending a variant of the received signal to the intended destination. It is necessary to specify which functionalities a relay node performs. In particular, relays can be categorized based on how the received signal is processed.

Amplify-and-Forward (AF) Relaying

From the signal processing perspective, a good signal processing algorithm employed at the relay should benefit the system's performance. Among many relaying approaches,

the Amplify-and-Forward (AF) relaying is the most basic and extensively studied. The structure of AF relaying is illustrated in Fig. 2.5, where the relay node simply amplifies the received signal from a source node and forwards the result to the destination. An AF relay operates at the physical layer and can be applied to any wireless infrastructure, thanks to its independence from both the system's coding method and modulation type.

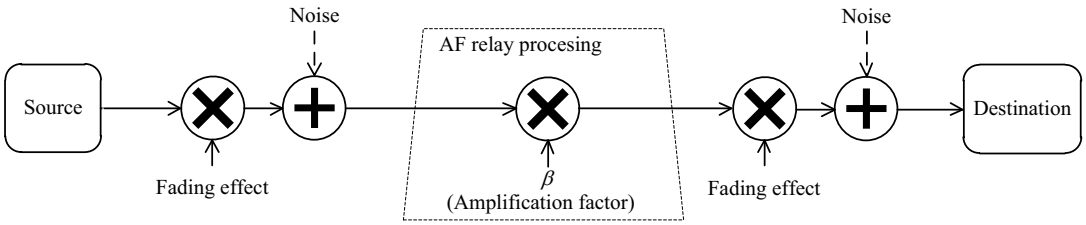

Figure 2.5 Amplify-and-Forward relaying.

Decode-and-Forward (DF) Relaying

An alternative to AF relaying is Decode-and-Forward (DF) relaying, which is illustrated in Fig. 2.6. While an AF relay retransmits the amplified signal without decoding, a DF relay decodes the received signal, encodes the result, and re-transmits. A DF relay's functionalities therefore are more complicated than the simple amplification done in an AF relay. In fact, a DF relay acts like a separated destination node, but is typically closer to the source. Relative to an AF relay, a DF relay can avoid noise accumulation when it successfully decodes the source's information. On the other hand, if the signal is not correctly decoded, a DF relay still forwards erroneous messages to the destination and it is unlikely that the receiver at the destination can recover the original information.

Other Relaying Strategies

Nevertheless, for a specific system configuration, neither AF nor DF is the best relaying strategy. As such, many other relaying strategies have been studied, including Compress-and-Forward [32], Partial Decode-and-Forward [29], Adaptive Decode-and-Forward and Hybrid AF/DF [33], etc. It should also be pointed out that many studies suggest the best location

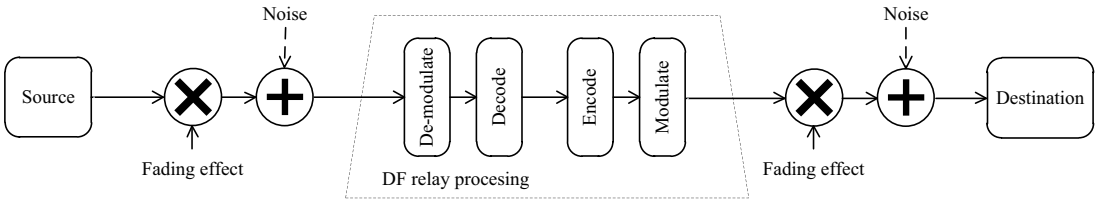

Figure 2.6 Decode-and-Forward relaying.

to position a relay is midway between the source and the destination.

This thesis focuses on the Partial Decode-and-Forward (PDAF) relaying which is firstly introduced in [29]. In particular, the relay only needs to realize and forward suitable composite multiuser signals, as opposed to complete decoding of every user's message as in the DF strategy. More details of PDAF relaying will be described in the next chapter.

2.2 Fading and Frequency Hopping Spread Spectrum

Fading, which is generated from the so-called multi-path propagation, is one of the most challenging problems in the design of a wireless communication system. Unlike wired communications where there is a fixed transmission medium to carry signals, in wireless communication, the channel between a transmitter and a receiver keeps changing rapidly over time. Usually a transmitted signal not only comes to a destination via a direct path but is also routed along other paths, created by reflection, which may have different amounts of attenuation and phase shift. Often fading reduces transmission quality, but such degradation can be mitigated by implementing an equalizer at each receiver. However, there is a situation in which reflected waves have unfavorable phases and amplitudes that they add up destructively and cancel out each other. This detrimental effect is often referred to as deep fading which may results in temporary failure of communications due to the severe drops in the received signal's power (see Fig. 2.7). Fading also depends on multi-path distances between the transmitter and the receiver. Therefore, adjusting the receiver's location could improve signal quality. However, if both the transmitter and receiver are fixed stations or slowly-moving, counteracting deep fading is not an easy task.

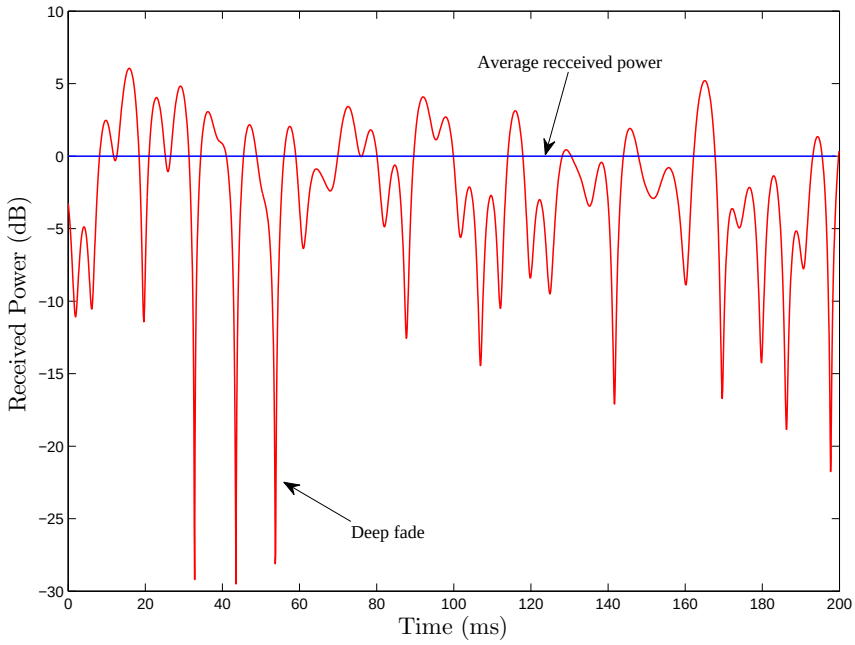

Figure 2.7 Example of deep fades in a Rayleigh fading channel

Fortunately, fading also depends on the carrier frequency which influences phases of multi-path signals received at the destination. It is shown that frequencies separated by a coherence bandwidth experience independent fading [34]. Therefore, sequentially changing the frequency from one channel to another might possibly improve communication quality from very poor to very good. This observation inspires the technique of *frequency hopping* (FH).

Early application of the FH technique was found in the Global System for Mobile Communications (GSM), specified by European Telecommunications Standards Institute (ETSI). In GSM, one carrier frequency is organized into eight basic physical channels, each of which has different time slot (TDMA scheme). A single physical channel can be assigned to one link between a mobile and a base station. The transmission between the mobile and the base station occurs in bursts within the designated time slot, which lasts about 576.9 μs [35]. There are also other carrier frequencies available, under a condition that any two adjacent carriers must be separated by at least 200 kHz. When FH is used, the carrier frequency may be changed between consecutive TDMA frames. That is, the mobile transmits on a fixed frequency during one time slot and then hops to another frequency before transmission of the

next frame. When frequency hopping is done on the burst basis, it is called *Slow Frequency Hopping* (SFH), because more than one symbol is transmitted using the same frequency.

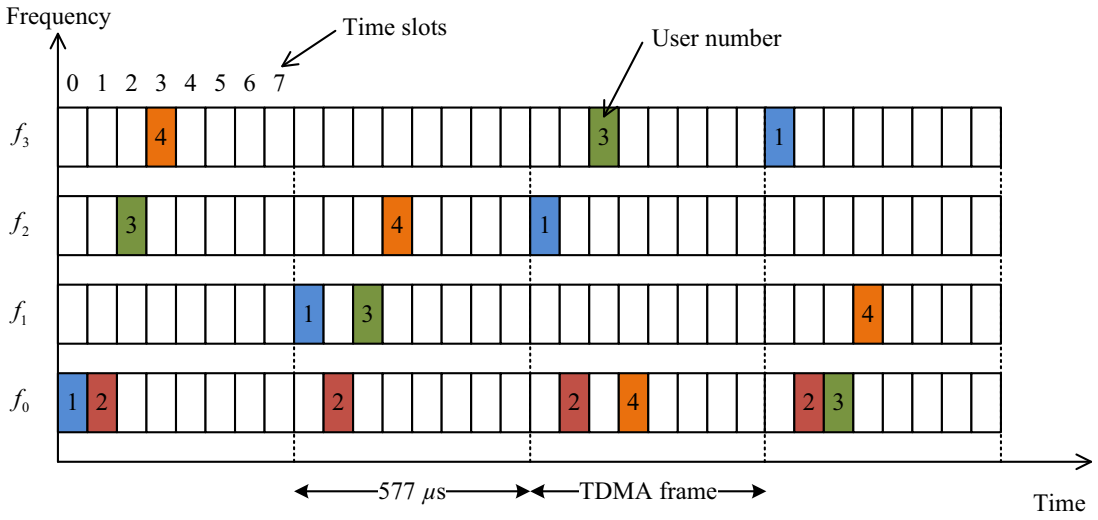

Figure 2.8 Example of Slow-Frequency-Hopping in GSM

Fig. 2.8 gives an example of GSM SFH scheme with 4 carriers.[1] Determined by a control unit, the carrier frequencies can be switched according to a certain rule. When the FH mode is deactivated, a mobile user only sends its data burst on one carrier (for example, user 2 shown in Fig. 2.8). In the FH mode, the carrier frequency keeps changing over individual TDMA frames in a pseudo-random manner. The purposes are to provide frequency diversity and lower the overall likelihood of having consecutive errors in deep fade situations. Another benefit of using a pseudo random frequency hopping strategy is that it is possible to have multiple wireless links transmitting autonomously on top of each other, provided that they use different random key sequences and incorporate forward error correction so that the lost packets could be reconstructed.

[1]The GSM standard supports a maximum number of 64 consecutive frequencies.

2.3 Fast Frequency Hopping and Non-coherent Detection

Extending the concept of FH, *fast frequency hopping* (FFH) was investigated in [24], in which the carrier frequency is allowed to change more than once during a symbol duration. However this technique was not widely implemented in civilian applications at first. During the first and second World Wars, the FFH technique was primarily used in military applications in order to secure the confidential information and to make the system robust against jamming. Over the past few decades, FFH has gained considerable interest due to its robustness in multiple access (MA) channel. The first Frequency Hopping Multiple Access (FHMA) communication system was proposed by Cooper and Nettleton in 1978 [36], which uses Differential Phase-Shift Keying (DPSK) for wireless transmissions. In the following year, Viterbi introduced the use of M-ary Frequency Shift Keying (M-FSK) for low-rate multiple access mobile satellite systems [37]. Since it enables non-coherent detection, the M-FSK modulation has been widely adopted in Fast Frequency Hopping Multiple Access (FFH-MA) systems. The FFH M-FSK technique is also adopted as the modulation scheme for the relay systems considered in our research.

2.3.1 FFH-MA Communication System

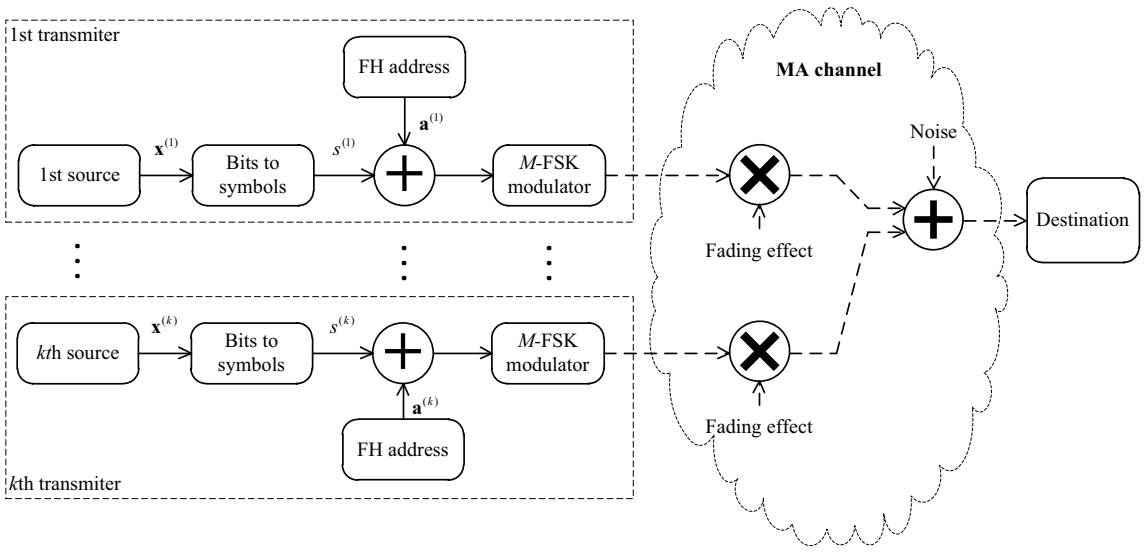

Figure 2.9 Structure of a FFH-MA communication system.

Fig. 2.9 shows a FFH-MA system model, including multiple FFH-MFSK transmitters. Each transmitted signal consists of L tones which are selected from M possible frequencies. Assume there are K users in the system, who transmit their signals simultaneously. Without loss of generality, the transmission of a symbol from the kth ($1 \leq k \leq K$) user is described. At first, the bit stream $\mathbf{x}^{(k)} = [x_0^{(k)}, x_1^{(k)}, \ldots, x_{q-1}^{(k)}]$ is converted to a M-FSK symbol by grouping $q = \log_2 M$ information bits together:

$$s^{(k)} = \sum_{i=0}^{q-1} x_i^{(k)} 2^i \tag{2.1}$$

This M-FSK symbol determines which frequency tones the are activated. The symbol transmission time T_s is divided into L time slots (also known as chip times), each of which has duration $T_c = T_s/L$. To maintain orthogonality among FSK frequencies, the minimum separation among any two adjacent frequency tones is $1/T_c$. Therefore the minimum bandwidth requirement for this system is M/T_c.

The challenging aspect of designing a FFH-MFSK system is to choose users' unique frequency hopping addresses. Since multiuser signals are overlapped in both time and frequency domains, their unique addresses are the key to distinguish one signal from others. Specifically, each user needs to switch frequency after each chip time and the next hop will be determined by its address code and transmitted symbol. The address code $\mathbf{a}^{(k)} = \left[a_0^{(k)}, a_1^{(k)}, \ldots, a_{L-1}^{(k)}\right]$ of the kth user has L components $\{a_l^{(k)}\}$, which belong to Galois Field GF(M). Then $\mathbf{a}^{(k)}$ is combined with the transmitted symbol $s^{(k)}$ to create time-frequency (TF) matrix $\mathbf{S}^{(k)}$, which is used to decide which frequency tone is activated at a particular chip time. The entries of matrix $\mathbf{S}^{(k)}$ are determined as

$$\left[\mathbf{S}^{(k)}\right]_{m,l} \equiv S_{m,l}^{(k)} = \begin{cases} 1, & \text{if } s^{(k)} \oplus a_l^{(k)} = m \\ 0, & \text{otherwise} \end{cases}, \tag{2.2}$$

where $m = 0, 1, \ldots, M-1$, $l = 0, 1, \ldots, L-1$ and $\oplus$ denotes addition in Galois Field GF(M). Thus $\mathbf{S}_n^{(k)}$ is a binary matrix, whose columns correspond to chip times and whose rows correspond to the sub-band frequencies.

All users transmit *simultaneously* to the destination over the same frequency band. In general, the FH addresses of different users are not orthogonal, hence interference among

users exists. For example, it is always possible to have $S_{m,l}^{(i)} = S_{m,l}^{(j)}$ for certain values of m and l with $i \neq j$. The amount of interference depends on how the FH address codes are designed. The selection of the address code might be such that the components of $\mathbf{a}^{(k)}$ are chosen at random or according to some specific method. Although randomly-generated FH addresses can be used, it is known that Einarsson's design method [38] minimizes the chance of having frequency collision among multiple users. Extensive computer simulations in [39] have supported Einarsson's proposal and this method is still being considered as the optimum choice for generating FH address codes.

Fig. 2.10 gives a visual illustration of different assignments of FH addresses and their effects on transmission performance (in terms of diversity and interference). In this example, the parameters M, L, K are set equal to $8, 4$ and 2, respectively. Comparison among 3 design methods are shown with their respective TF matrices. Users' transmitted symbols are $s^{(1)} = 2$ and $s^{(2)} = 3$. It is pointed out that in a communication system, error rate is highly influenced by the worst case scenario. Therefore only the most error-prone situation associated with each design is shown in the figure. The following observations are made:

- In the "bad design", $\mathbf{a}^{(1)} = [1, 1, 2, 3]$ and $\mathbf{a}^{(2)} = [0, 0, 0, 0]$. It can be seen that there are maximum two collisions that occur when two users send the same frequency tones in the first two chip times. Signals from two users coming from different paths might add up destructively and cause *erasures* (elimination of signals at destination) or might add up constructively and generate a near-far effect, which reduces the receiver's performance.

- In the "good design", $\mathbf{a}^{(1)} = [0, 1, 2, 3]$ and $\mathbf{a}^{(2)} = [0, 0, 0, 0]$. It is obvious that the choice of FH addresses allows a maximum one frequency coincidence for any given values of $s^{(1)}$ and $s^{(2)}$. However, signal from the second user does not have frequency diversity and it occupies completely one sub-band during a symbol transmission. Such a signal will suffer a severe degradation in a multi-path fading channel. For the address scheme of the first user, its *linear* address assignment is not good either. This is because the fading effect can spread over several local consecutive frequencies. In fact, it is always better to spread the user's frequency tones over entire available bandwidth, i.e., keep

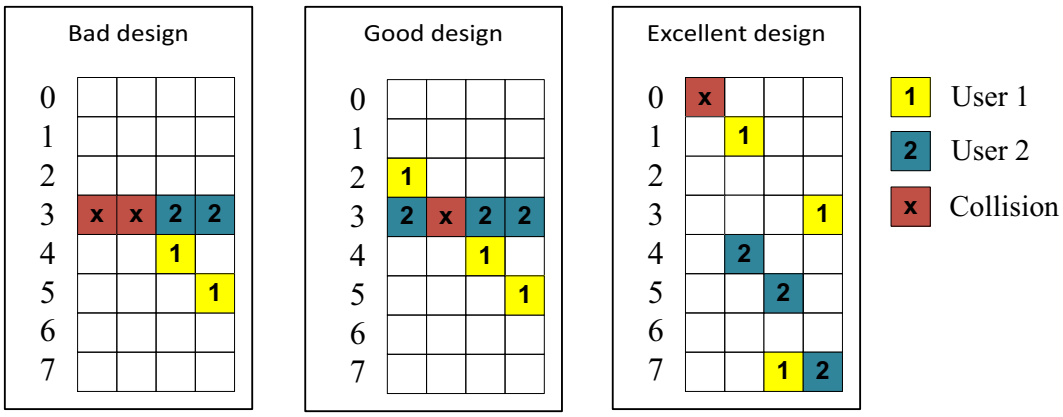

Figure 2.10 An example of different designs of frequency hopping addresses.

them further away from each other as much as possible.

- In the "excellent design", $\mathbf{a}^{(1)} = [6, 7, 5, 1]$ and $\mathbf{a}^{(2)} = [5, 1, 2, 4]$ [38]. One can see that not only the probability of collision is minimized (maximum 1 for 2 users, 2 for 3 users and so on), but also the time-frequency diversity is well maintained among all users.

2.3.2 Conventional Detection of FFH Signals

The conventional FFH detector shown in Fig. 2.11 is also referred to as a majority logic decoder [40], which can provide estimation for one or several desired users. The front-end of such a detector contains a M-FSK demodulator, which reverses the operation of the M-FSK modulator. Specifically, it contains a bank of M non-coherent detectors (also known as energy detectors or squared-law detectors) that tune to the M possible frequency tones. Each squared-law detector measures the energy contains in one particular chip over the duration T_c. Each output is then compared to a *threshold* (hard detected): if the output exceeds this threshold, the detector output is 1, yielding a non-zero entry in the received observation matrix $\mathbf{R}$. Thus, $\mathbf{R}$ is a binary matrix with its TF locations marked "0" or "1" depending on whether there is an user who activates that location or not. On a *perfect* channel where neither noise nor fading is present, the "optimal" matrix $\mathbf{R}^{(\text{opt})}$ is obtained by performing

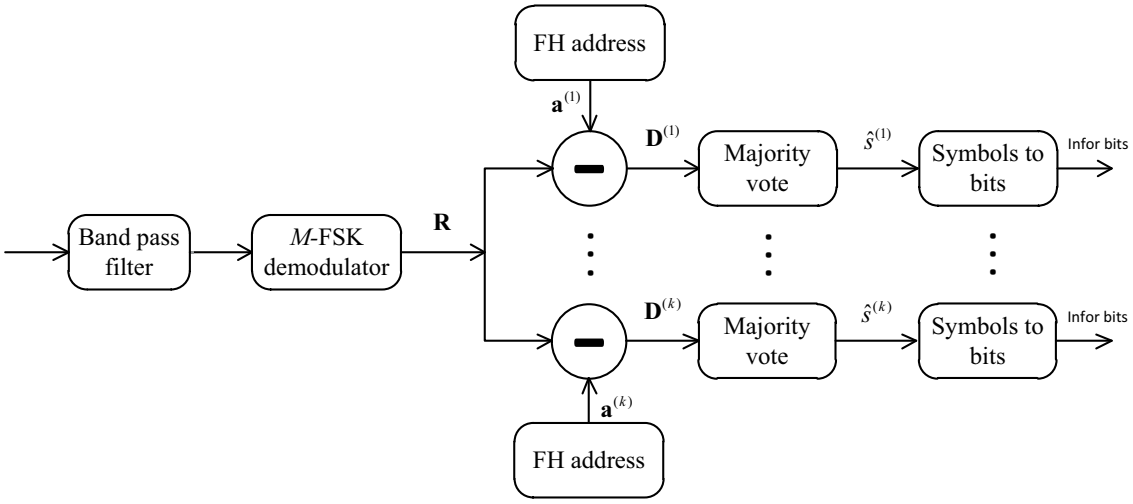

Figure 2.11 Conventional FFH detector.

logical OR on all binary matrices $\{\mathbf{S}^{(k)}\}_{k=1}^{K}$:

$$\left[\mathbf{R}^{(\text{opt})}\right]_{m,l} \equiv R_{m,l}^{(\text{opt})} = \bigvee_{k=1}^{K} S_{m,l}^{(k)}, \tag{2.3}$$

where $m = 0, 1, \ldots, M-1$, $l = 0, 1, \ldots, L-1$ and $\bigvee$ denotes the logical OR operation. In real transmission, false alarm occurs when a chip is not actually activated but the noise level exceeds the decision threshold. On the other hand, there is also a possibility of miss detection when the detected power drops below the threshold due to severe fading or frequency conflict between two users. In general, the matrix $\mathbf{R}$ of M-FSK demodulator might differ with the ideal result in (2.3) and the number of different entries would depend on the channel condition.

The next step is to obtain the user-specific de-spreading matrix for symbol detection of the desired user. Depending on each user's unique FH address $\mathbf{a}^{(k)}$, the de-spreading matrix $\mathbf{D}^{(k)}$ can be taken from the observation matrix as follows:

$$\left[\mathbf{D}^{(k)}\right]_{m,l} \equiv D_{m,l}^{(k)} = R_{\hat{m},l}, \tag{2.4}$$

where $\hat{m} = m \oplus a_l^{(k)}$. Then the majority vote is performed on $\mathbf{D}^{(k)}$ to find symbol $\hat{s}^{(k)}$ that is

most likely to be sent by the kth user. The rule to decide is: *Choose the codeword associated with the row containing the greatest number of entries* [40].

Fig. 2.12 gives an illustration of de-spreading matrices in the detection process. The parameters in this example are obtained from the excellent FH address design mentioned on Page 19. In the figure, shaded boxes refer to locations that are marked "1" in the associated binary TF matrix. As can be seen, noise and multi-path propagation can influence the de-spreading matrices. While the symbol from user 1 is detected correctly with one full row indicating $\hat{s}^{(1)} = 2$, detection of user 2 has an ambiguity between $\hat{s}^{(2)} = 3$ and $\hat{s}^{(2)} = 5$, which is caused by energy deletion and occurrence of the false alarm.

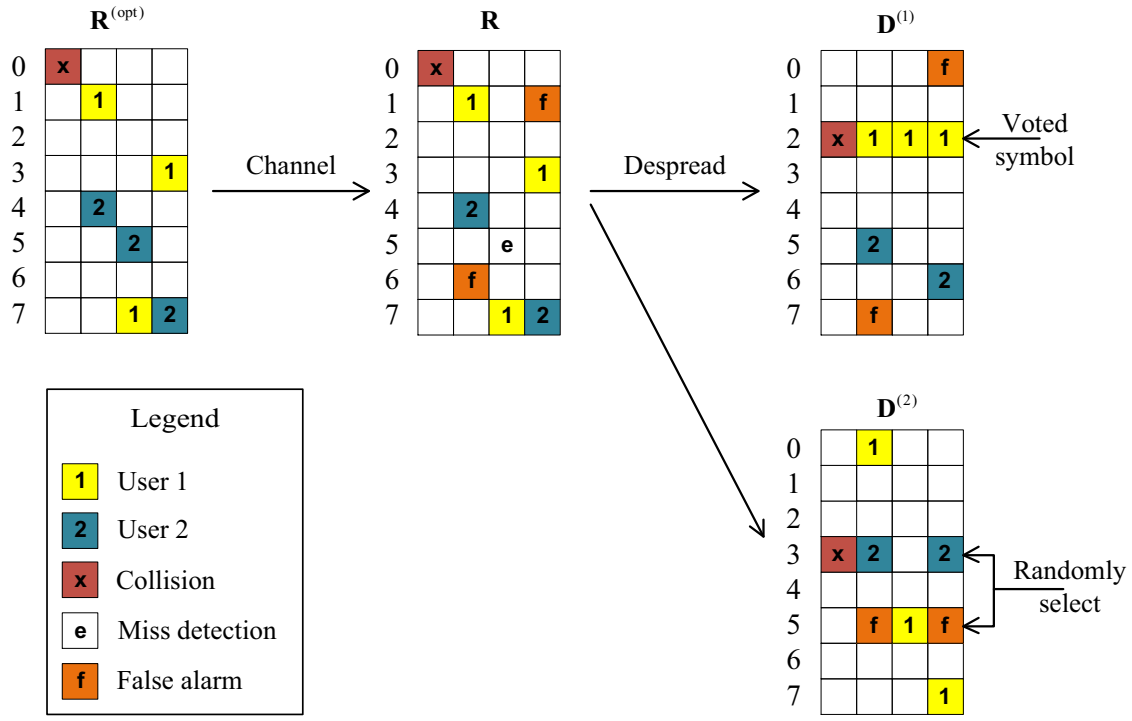

Figure 2.12 TF matrices at destination.

2.3.3 Joint Maximum Likelihood Detection

As the name suggests, this method jointly detects signals from all users at once by measuring the coincidence among the received matrix $\mathbf{R}$ and candidate matrices generated

from a joint K-users symbol space [41]. Specifically, first it requires the generation of $\mathbf{s} = [s^{(1)}, s^{(2)}, \ldots, s^{(K)}]$ that contains all distinct combinations of all K users' transmitted symbols. In total, there would be M^K possibilities of choosing $\mathbf{s}$. For each possibility, $\mathbf{U_s}$ is obtained by performing the logical OR over the distinct combinations of all K users' transmit matrices $\mathbf{S}^{(k)}$:

$$[\mathbf{U_s}]_{m,l} \equiv \mathbf{U}_{\mathbf{s},m,l} = \bigvee_{k=1}^{K} S_{m,l}^{(k)}, \text{ given that } s^{(k)} = \mathbf{s}(k), \ \forall k = 1, 2, \ldots, K. \tag{2.5}$$

Then a cost function is defined by counting the number of coinciding elements between $\mathbf{U_s}$ and $\mathbf{R}$:

$$f(\mathbf{s}) = \sum_{m=0}^{M-1} \sum_{l=0}^{L-1} U_{\mathbf{s},m,l} \times R_{m,l}. \tag{2.6}$$

Finally, the ML joint detection is performed by maximizing $f(\mathbf{s})$ over all M^K possible patterns of $\mathbf{s}$. Since M^K is an extremely large number, even for a system with a moderate number of users, the huge complexity of this method makes it impractical. This difficulty motivates a low-complexity algorithm as discussed in the following section.

2.3.4 Iterative Interference Cancellation (IIC)

While the idea of iterative cancellation of multi-user interference has widely been applied to CDMA systems, there is little effort in applying IIC to FFH systems. In 1996, Fiebig [42] first introduced a low-complexity algorithm for the joint detection of FFH signals in MA channels. The principle of the algorithm starts with the conventional detection where symbol decisions are carried out if the corresponding de-spreading matrices do not contain ambiguities. Taking into account these symbol decisions, the corresponding entries in the received matrix $\mathbf{R}$ are canceled (erased) and the conventional detection process is re-invoked based on a modified received matrix. Then the process is iteratively carried out until either all symbols are estimated or the last iteration does not yield a further symbol decision. Fiebig [42] provides visual illustrations of this algorithm, and also derives a tight bound on the bit error probability of this detection method.

Few years later, Fiebig and Roberson [43] proposed soft decoding for the FFH-MFSK systems, which gives the opportunity to incorporate advanced channel encoders/ decoders. According to their research, although soft information is obtained from the 2-level hard-

limited received matrix $\mathbf{R}$, their proposed soft-decoding method gives a much better performance than using hard decoding. This idea is then expanded by Park and Lee [44] by incorporating iterative decoding techniques to the coded FFH-MFSK system in order to improve the channel capacity. They also consider 3-level hard-limited decision instead of the conventional 2-level decision and show that it helps improve the performance slightly.

However, the hard-limiting operation applied on the received signals is clearly sub-optimal as it throws away part of the information delivered to the destination. Inspired by the previous works and based on this observation, the next chapter proposes and analyzes a novel IIC algorithm that makes full use of the received signals at the destination.

3. Multi-User Relaying System with FFH Modulation

3.1 Introduction

As discussed in Chapter 2, FFH modulation has many good features and has been studied by many researchers (see, for example [25, 43, 45–49]). The main advantage of FFH modulation is that it is highly tolerant to narrow-band interference as well as burst noise. Using a relatively simple interference avoidance technique which provides time-frequency diversity, an FFH system can share the same frequency band with another system using different modulation type [50]. Such a feature also makes FFH modulation technique suitable for MA communications. Furthermore, in combination with non-coherent detection, the FFH demodulator can be strongly resistant to phase noise and simple to implement. The analysis of FFH modulation in a MA system was first performed in [40], which takes into account many factors such as bandwidth, transmission rate, number of users, noise and interference issues. The authors also proposed an optimal design under the assumption of random user address assignment. Later on, Einarsson [38] investigated an optimal address assignment to minimize the interference in a FFH-MA system. An upper bound on the bit error rate (BER) versus the number of users in the system was also provided.

The existence of MAI, caused by the non-orthogonality of FH addresses, is an inherent issue of an FFH-MA system. The MAI cannot be completely suppressed by the receiver and is the main source of performance degradation. In general, the level of MAI can be reduced by increasing the hopping rate at the expense of a reduced data rate. Different approaches have also been developed to deal with the MAI issue without sacrificing the data rate. One approach was initially presented in [42] in which the author developed an iterative multiuser

detector (MUD) that exploits the prior knowledge of the FH addresses and energies of the user signals for interference cancellation. Specifically, by taking into account the imbalance of the instantaneous signal levels among multiple users, those signals with a better chance of being detected correctly are decoded first and the results are used to remove the ambiguity for detecting signals experiencing higher level of interference. This ideas was later extended in [51] with the introduction of a multistage multiuser detector. When channel coding is used, different strategies are investigated to deal with MAI by incorporating the outputs of the channel decoders in the interference cancellation process [44, 47, 52].

Most of research contributions in the area of FFH modulation focus on point-to-point transmission, while only a few studies consider relay-assisted transmission framework. Recently a multiuser relaying communication scheme based on FFH-MA was presented in [29]. Making use of the half-duplex two-phase communication protocol, it was shown that a relay can help to improve the channel quality at the expense of reducing the transmission rate by half. An optimal maximum-likelihood multiuser detector (ML-MUD) was obtained and shown to achieve a good performance. However, the complexity of the ML-MUD grows exponentially with the number of users and frequency tones [25], thus making it very expensive, if not impossible, for practical implementation.

The system model presented in this chapter is similar to that in [29], i.e., it is concerned with multiuser relaying with the help of a single relay. The difference is that, while [29] only focuses on the demodulation of uncoded information transmission, channel coding is considered in this thesis. By exploiting channel coding, an iterative receiver is developed for both cases of AF relaying and PDAF relaying. In both cases, the complexity of the iterative receiver is only proportional to the numbers of users and frequency tones. The key operation of the developed receiver is to successively extract the maximum likelihood symbols of users and use that information for interference cancellation. Simulation results demonstrate performance improvement with iterations and the superiority of the proposed receiver when compared with the detection method in [29] under the same spectral efficiency.

The rest of this chapter is organized as follows. Section 3.2 details the system model under consideration. The calculations needed for interference cancellation in the iterative

receiver are provided in Section 3.3. Section 3.4 presents and discusses simulation results.

3.2 System Model

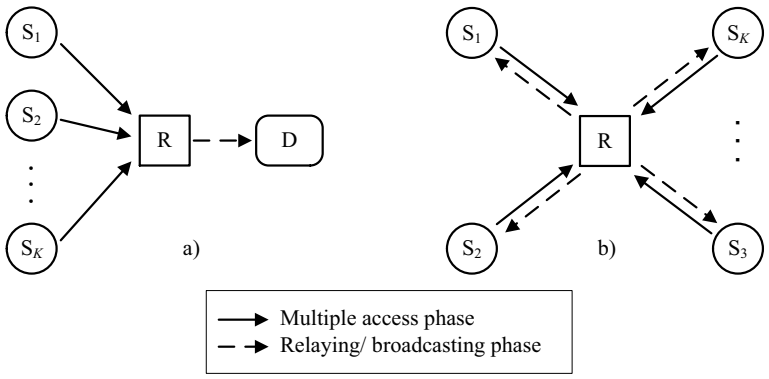

Figure 3.1 Two models of relay networks: (a) Multiuser one-way relaying and (b) Multiuser multi-way relaying.

Fig. 3.1-(a) illustrates a wireless network in which K users wish to send their information to a destination with the help of a relay. The relay operates in a half-duplex mode, i.e., it can only transmit or receive at any given time. As such, transmission of information from users to the destination happens in two phases. In the first phase, all users send their information to the relay. The relay performs some form of signal processing on the received signal before sending a new signal to the destination in the second phase. Upon receiving the signal from the relay, the destination needs to detect the information for all K users. Note that such a relay network is closely related to the *multi-way* relaying considered in [29], which is depicted in Fig. 3.1-(b). Compared to multiuser one-way relaying, the major difference of multiuser multi-way relaying is that, instead of a single receiver, there are K receivers, one at each user to detect information from the $K-1$ other users. Naturally, the receiver developed in this chapter for one-way relaying can be readily applied for each user in multi-way relaying by subtracting out its own information.

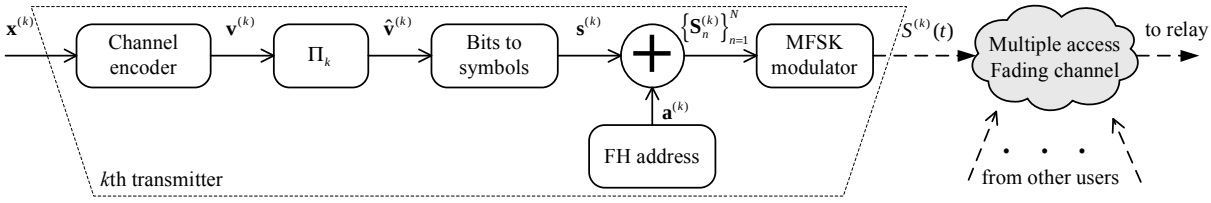

Figure 3.2 Structure of the kth user's transmitter.

3.2.1 Information Transmission of Users

Fig. 3.2 illustrates the transmitter's structure for the kth user. First, a vector of N_i information bits, $\mathbf{x}^{(k)}$, is encoded into a codeword $\mathbf{v}^{(k)}$. An interleaver Π_k, specific to each user, is performed on $\mathbf{v}^{(k)}$ to produce the interleaved codeword $\hat{\mathbf{v}}^{(k)}$. The interleaved codeword $\hat{\mathbf{v}}^{(k)}$ is then modulated into a frame of N symbols, $\mathbf{s}^{(k)} = [s_0^{(k)}, s_1^{(k)}, \ldots, s_{N-1}^{(k)}]$. Here, $N = \frac{N_i R_c}{q}$, where R_c is the code rate and $q = \log_2 M$ is the number of bits per M-ary frequency shift keying (M-FSK) symbol. For transmission with FFH, the symbol period T_s is split into L chip times, each with a duration of $T_c = T_s/L$. Each user is assigned a unique FH address, $\mathbf{a}^{(k)} = \left[a_0^{(k)}, a_1^{(k)}, \ldots, a_{L-1}^{(k)}\right]$. For each symbol $s_n^{(k)}$, $n = 0, 1, \ldots, N-1$, a $M \times L$ time-frequency (TF) matrix $\mathbf{S}_n^{(k)}$ is formed to determine which frequency (i.e., sub-band) is activated at a particular chip time. The entries of matrix $\mathbf{S}_n^{(k)}$ are determined as

$$\left[\mathbf{S}_n^{(k)}\right]_{m,l} \equiv S_{n,m,l}^{(k)} = \begin{cases} 1, & \text{if } s_n^{(k)} \oplus a_l^{(k)} = m \\ 0, & \text{otherwise} \end{cases}, \tag{3.1}$$

where $m = 0, 1, \ldots, M-1$, $l = 0, 1, \ldots, L-1$ and $\oplus$ denotes addition in Galois Field GF(M). Thus $\mathbf{S}_n^{(k)}$ is a binary matrix, whose columns correspond to chip times and whose rows correspond to the sub-band frequencies.

In the first phase, i.e., the multiple-access phase, all users transmit *simultaneously* to the relay over the same frequency band. In general, the FH addresses of different users are not orthogonal, hence interference among users exists. For example, it is always possible to have $S_{n,m,l}^{(i)} = S_{n,m,l}^{(j)}$ for certain values of m and l with $i \neq j$. The amount of interference depends on how the FH address codes are designed. Although randomly-generated FH addresses can be used, it is known that Einarsson's design method [38] minimizes the chance of having

frequency collision among multiple users. This method shall also be used to assign FH addresses of users in this chapter.

The complex baseband-equivalent transmitted signal from the kth user over one frame duration (i.e., N symbol durations) can be expressed as follows

$$S^{(k)}(t) = \sqrt{\frac{2E_c}{T_c}} \sum_{n=0}^{N-1} \sum_{l=0}^{L-1} \exp\left(j2\pi f_{n,l}^{(k)} t + \theta_{n,l}^{(k)}\right) \psi(t - lT_c - nT_s), \quad 0 \le t \le NT_s, \tag{3.2}$$

where E_c is the transmitted energy per chip, $\psi(t)$ is a rectangular pulse shaping function of unit amplitude over $0 \le t \le T_c$ and zero otherwise. The set of frequency tones $f_{n,l}^{(k)}$ is determined by the *nonzero* entries in $\mathbf{S}_n^{(k)}$. Since it is desired to maintain the orthogonality across multiples tones within a chip time duration, two adjacent sub-bands need to be separated by at least $1/T_c$. Specifically, if $S_{n,m,l}^{(k)} = 1$, then the frequency tone of the kth user during the interval $lT_c + nT_s \le t < (l+1)T_c + nT_s$ is $f_{n,l}^{(k)} = \frac{m}{T_c}$. Moreover, the phases of all the active carriers, $\theta_{n,l}^{(k)}$, are treated as independent uniform random variables over $(0, 2\pi)$. Note that the transmitted power of the signal in (3.2) is $P_{\text{tx}}^{(k)} = 2E_c/T_c$.

With synchronous transmissions of all the users over the frequency-flat Rayleigh fading channels, the complex baseband-equivalent signal received at the relay during the MA phase can be written as follows:

$$R(t) = \sqrt{\frac{2E_c}{T_c}} \sum_{k=1}^{K} \sum_{n=0}^{N-1} \sum_{l=0}^{L-1} h_{n,l}^{(k)} \psi(t - lT_c - nT_s) \exp\left(j2\pi f_{n,l}^{(k)} t\right) + w(t), \quad 0 \le t \le NT_s. \tag{3.3}$$

In (3.3), the phase term $\theta_{n,l}^{(k)}$ has been absorbed into the channel gain $h_{n,l}^{(k)}$, which is modeled as a zero-mean, unit-variance circularly-symmetric complex Gaussian random variable, i.e., $h_{n,l}^{(k)} \sim \mathcal{CN}(0,1)$. Furthermore, $h_{n,l}^{(k)}$ are independent across users and over different chip times [29]. The term $w(t)$ is complex additive white Gaussian noise (AWGN) with one-sided power spectrum density (PSD) N_0 per dimention. Note that, with the above signal model, the *received* signal-to-noise ratio (SNR) per information bit is

$$\gamma_b = \frac{LE_c}{R_c q N_0}. \tag{3.4}$$

As mentioned before, after receiving $R(t)$, the relay performs some form of signal processing on $R(t)$ to extract useful information, re-modulates and forwards a new signal to the

destination so that the destination can detect information bits of all K users. The following subsections consider two relaying options, namely (i) amplify-and-forward, and (ii) partially decode-and-forward.

3.2.2 Amplify-and-Forward Relaying

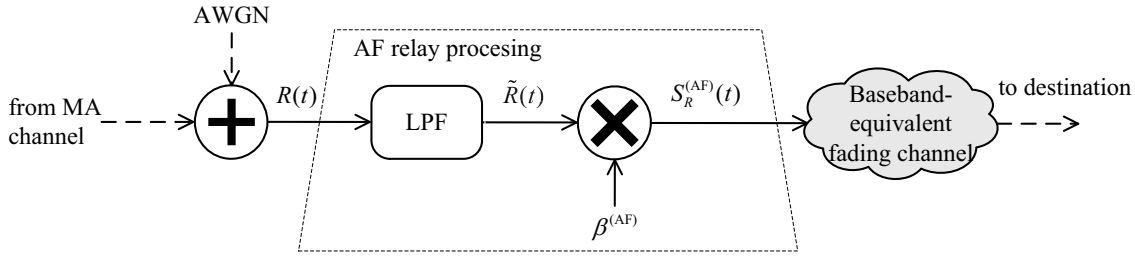

Figure 3.3 Structure of AF relaying.

Fig. 3.3 shows the structure of amplify-and-forward relaying in complex baseband-equivalent model. As the name suggests, the relay node simply filters and amplifies the received signal in the first transmission phase and forwards the amplified version to the destination in the second phase. The purpose of the low-pass filter (LPF) in Fig. 3.3 is to limit the bandwidth of AWGN to the bandwidth of users' transmitted signals, which is approximately $W = M/T_c$. Let $\tilde{R}(t)$ be the received signal after the LPF. Then $\tilde{R}(t)$ is composed of the same signal component, i.e., the first term in (3.3), and the complex band-limited noise $\tilde{w}(t)$, which has an average power of $\frac{2MN_0}{T_c}$.

Without loss of generality, let's focus on the received signal at the relay over one arbitrary chip duration in order to determine the amplification factor $\beta^{(\mathrm{AF})}$. Specifically, the received signal after the LPF during the lth chip interval of nth symbol can be written as follows

$$\begin{aligned}\tilde{R}_{n,l}(t) &= \sqrt{\frac{2E_c}{T_c}} \sum_{k=1}^{K} h_{n,l}^{(k)} \exp(j2\pi f_{n,l}^{(k)})t + \tilde{w}(t) \\ &= X_{n,l}(t) + \tilde{w}(t), \quad lT_c + nT_s \le t \le (l+1)T_c + nT_s,\end{aligned} \tag{3.5}$$

where $X_{n,l}(t)$ is the superimposed signal of all users. In order to maintain the transmitted

power of the relay to be $P_{\text{tx}}^{(\text{R})}$, the value of $\beta^{(\text{AF})}$ is:

$$\beta^{(\text{AF})} = \sqrt{\frac{P_{\text{tx}}^{(\text{R})}}{P_{\text{rx}}^{(\text{R})} + 2MN_0/T_c}}, \tag{3.6}$$

where $P_{\text{rx}}^{(\text{R})}$ is the power of the signal portion received at the relay.

Under the assumption that all the channel gains are i.i.d. $\mathcal{CN}(0,1)$, the quantity $P_{\text{rx}}^{(\text{R})}$ is formally calculated as

$$\begin{aligned} P_{\text{rx}}^{(\text{R})} &= \mathbb{E}_{\{h_{n,l}^{(k)}\}} \left\{ \frac{1}{T_c} \int_{lT_c+nT_s}^{(l+1)T_c+nT_s} |X_{n,l}(t)|^2 \mathrm{d}t \right\} \\ &= \mathbb{E}_{\{h_{n,l}^{(k)}\}} \left\{ \frac{2E_c}{T_c^2} \int_{lT_c+nT_s}^{(l+1)T_c+nT_s} \left| \sum_{k=1}^{K} h_{n,l}^{(k)} \exp(j2\pi f_{n,l}^{(k)} t) \right|^2 \mathrm{d}t \right\}. \end{aligned} \tag{3.7}$$

Note that with the FFH-MA scheme, there is a chance of having frequency collision, i.e., $f_{n,l}^{(i)} = f_{n,l}^{(j)}$, $1 \le i < j \le K$. On the other hand, since different carrier frequencies are made orthogonal over the chip interval T_c, all the cross-term components involving two or more carrier frequencies in (3.7) would evaluate to zero. Let $\mathcal{I}$ and $\mathcal{K}$ denote the sets of interfered users and non-interfered users, respectively, and let $\mathcal{I}[i]$ and $\mathcal{K}[i]$ refer to the ith elements in these respective sets. It then follows that (3.7) can be written as follows

$$\begin{aligned} P_{\text{rx}}^{(\text{R})} &= \frac{2E_c}{T_c^2}\, \mathbb{E}_{\{h_{n,l}^{(k)}\}} \left\{ \left| \sum_{i=1}^{I} h_{n,l}^{(\mathcal{I}[i])} \right|^2 \int_{lT_c+nT_s}^{(l+1)T_c+nT_s} \left| \exp(j2\pi f_{n,l}^{(\mathcal{I}[1])} t) \right|^2 \mathrm{d}t \right. \\ &\qquad \left. + \sum_{i=1}^{K-I} \left| h_{n,l}^{(\mathcal{K}[i])} \right|^2 \int_{lT_c+nT_s}^{(l+1)T_c+nT_s} \left| \exp(j2\pi f_{n,l}^{(\mathcal{K}[i])} t) \right|^2 \mathrm{d}t \right\} \\ &= \frac{2E_c}{T_c} \mathbb{E}_{\{h_{n,l}^{(k)}\}} \left\{ \left| \sum_{i=1}^{I} h_{n,l}^{(\mathcal{I}[i])} \right|^2 + \sum_{i=1}^{K-I} \left| h_{n,l}^{(\mathcal{K}[i])} \right|^2 \right\} = \frac{2KE_c}{T_c}, \end{aligned} \tag{3.8}$$

where I, $0 \le I \le K$ is number of elements in the set $\mathcal{I}$. Substituting (3.8) into (3.6) gives

$$\beta^{(\text{AF})} = \sqrt{\frac{T_c P_{\text{tx}}^{(\text{R})}}{2KE_c + 2MN_0}}. \tag{3.9}$$

For the case that the power of the relay is constrained to be the sum of all transmitted powers at the user nodes, i.e., $P_{tx}^{(R)} = KP_{tx}^{(k)}$, one has $\beta^{(\text{AF})} = \sqrt{\frac{KE_c}{KE_c + MN_0}}$.

Once $\beta^{(\text{AF})}$ is determined, the relay transmits signal $S_R^{(\text{AF})}(t) = \beta^{(\text{AF})} \tilde{R}(t)$ to the destination. The structure of the receiver at the destination is described in Section 3.2.4.

3.2.3 Partially Decode-and-Forward Relaying

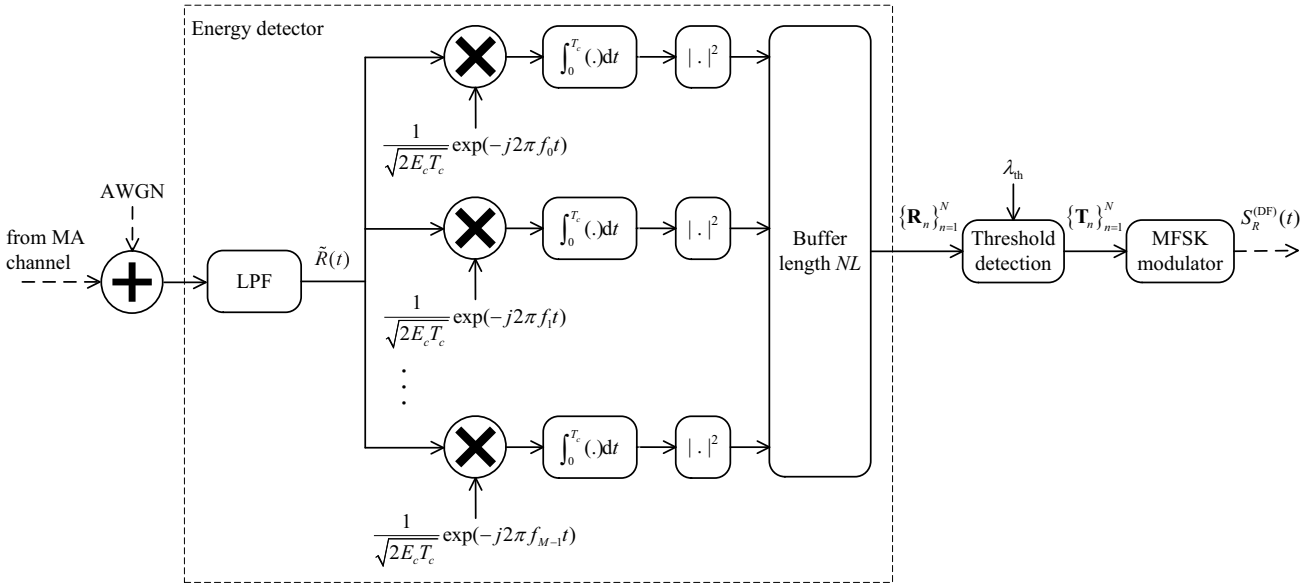

Figure 3.4 Structure of partial DF relaying.

As an alternative to the simple AF relaying, a partial DF relaying scheme is proposed in Fig. 3.4, in which an energy detector and a FSK modulator are introduced at the relay. The name "partial DF relaying" is used since the users' information bits are not fully decoded at the relay. The details of the partial DF relaying are described next.

First, an LPF is applied to received signal $R(t)$ in (3.3) to obtain band-limited signal $\tilde{R}(t)$. Over the nth symbol duration, $n = 0, 1, \ldots, N-1$, the relay performs energy detection on $\tilde{R}(t)$ to obtain a $M \times L$ normalized time-frequency matrix $\mathbf{R}_n$. The (m, l)th entry of $\mathbf{R}_n$ can be expressed as [29]

$$\begin{aligned} R_{n,m,l} &= \left| \frac{1}{T_c} \int_{lT_c+nT_s}^{(l+1)T_c+nT_s} \frac{\tilde{R}(t)}{\sqrt{2E_c/T_c}} \psi(t - lT_c - nT_s) \exp(-j2\pi f_m t) \mathrm{d}t \right|^2 \\ &= \left| \sum_{k=1}^{K} h_{n,l}^{(k)} \delta(f_{n,l}^{(k)} - f_m) + \tilde{w}_{n,m,l} \right|^2, \end{aligned} \tag{3.10}$$

where $\delta(\cdot)$ is the Dirac delta function, defined as $\delta(0) = 1$ and $\delta(x) = 0, \forall x \neq 0$, and $\tilde{w}_{n,m,l}$ is zero-mean complex AWGN component with variance $\sigma_{\tilde{w}}^2 = N_0/E_c$. Note that, since $h_{n,l}^{(k)}$ and $\tilde{w}_{n,m,l}$ are complex Gaussian random variables, it follows that $R_{n,m,l}$ obeys the exponential

distribution with mean $K_{n,m,l}+\sigma_{\tilde{w}}^2$, where $K_{n,m,l} \in \{0,1,\ldots,K\}$ is the number of users who activate the mth frequency tone during the lth chip time of the nth symbol duration.

In preparation for information forwarding to the destination, the relay compares the energy level at each TF location with a threshold λ_{th} to obtain a binary TF matrix $\mathbf{T}_n$. Thus, the (m,l)th entry of $\mathbf{T}_n$ is

$$T_{n,m,l} = \begin{cases} 1, & \text{if } R_{n,m,l} \geq \lambda_{\text{th}} \\ 0, & \text{otherwise} \end{cases}. \tag{3.11}$$

The bits contained in matrix $\mathbf{T}_n$ are then sent to the destination to indicate which sub-band was active in a given chip time of a symbol duration during the MA phase (which could be due to one or multiple users). Using M-FSK modulation, the baseband-equivalent signal transmitted by the relay over one frame duration (N symbols) can be expressed as

$$S_R^{(\text{DF})}(t) = \beta^{(\text{DF})}\sqrt{\frac{2E_c}{T_c}}\sum_{n=0}^{N-1}\sum_{l=0}^{L-1}\sum_{m=0}^{M-1}\delta(T_{n,m,l}-1)\psi(t-lT_c-nT_s)\cdot\exp\left(j2\pi f_m t\right), \quad 0 \leq t \leq NT_s, \tag{3.12}$$

where the amplification factor $\beta^{(\text{DF})}$ is determined to maintain the relay's transmitted power to be $P_{\text{tx}}^{(\text{R})}$.

In general, the value of $\beta^{(\text{DF})}$ depends on system parameters K, M, L, as well as the choice of threshold λ_{th} at the relay. It is obvious that if λ_{th} is increased, the number of locations with value 1 in $\mathbf{T}_n$ reduces, hence more transmit power is spent on each activated chip duration. Assuming that the values of the TF matrix $\mathbf{T}_n$ are independent, the average transmitted power at the relay can be obtained as follows:

$$\begin{aligned} P_{\text{tx}}^{(\text{R})} &= \mathbb{E}\left\{\frac{1}{NT_s}\int_0^{NT_s}\left|S_R^{(\text{DF})}(t)\right|^2 \mathrm{d}t\right\} \\ &= \mathbb{E}\left\{\left(\beta^{(\text{DF})}\right)^2\frac{2E_c}{T_c}\frac{1}{NL}\sum_{n=0}^{N-1}\sum_{l=0}^{L-1}\sum_{m=0}^{M-1}\delta(T_{n,m,l}-1)\right\} \\ &= \left(\beta^{(\text{DF})}\right)^2\frac{2ME_c}{T_c}P(T_{n,m,l}=1) \\ &= \left(\beta^{(\text{DF})}\right)^2\frac{2ME_c}{T_c}P(R_{n,m,l}\geq\lambda_{\text{th}}). \end{aligned} \tag{3.13}$$

Recall that $R_{n,m,l}$ has an exponential distribution with a mean value determined by the number of users who activate the mth frequency tone. For a given chip duration, there are total K users; each of which can activate a particular frequency tone with equal probability $1/M$. Therefore, by applying the law of total probability, one has

$$\begin{aligned} P(R_{n,m,l} \geq \lambda_{\text{th}}) &= \sum_{k=0}^{K} P(R_{n,m,l} \geq \lambda_{\text{th}} | K_{n,m,l} = k) P(K_{n,m,l} = k) \\ &= \sum_{k=0}^{K} \exp\left(-\frac{\lambda_{\text{th}}}{k + \sigma_{\tilde{w}}^2}\right) B(K, k, 1/M), \end{aligned} \tag{3.14}$$

where $B(\cdot)$ is a binomial distribution, given as

$$B(K, k, 1/M) = \binom{K}{k} \frac{1}{M^k} \left(1 - \frac{1}{M}\right)^{(K-k)}. \tag{3.15}$$

Finally, substituting (3.14) into (3.13) gives

$$\beta^{(\text{DF})} = \sqrt{\frac{T_c P_{\text{tx}}^{(\text{R})}}{2ME_c \sum_{k=0}^{K} \exp\left(-\frac{\lambda_{\text{th}}}{k+\sigma_{\tilde{w}}^2}\right) B(K, k, 1/M)}}. \tag{3.16}$$

Before closing this section, it is relevant to discuss the choice of threshold λ_{th} used at the partial DF relay. First, consider the case of no interference (i.e., $K_{n,m,l} = 0$ or 1). In this situation, each entry $R_{n,m,l}$ has an exponential distribution with mean value of $(1 + \sigma_{\tilde{w}}^2)$ or $\sigma_{\tilde{w}}^2$, depending on whether there is a signal component at the (m, l)th location. The error probability of the squared-law detector using threshold λ_{th} is

$$\begin{aligned} P_e &= \frac{1}{2} P(\text{error} | K_{n,m,l} = 0) + \frac{1}{2} P(\text{error} | K_{n,m,l} = 1) \\ &= \frac{1}{2} \exp\left(-\frac{\lambda_{\text{th}}}{\sigma_{\tilde{w}}^2}\right) + \frac{1}{2}\left[1 - \exp\left(-\frac{\lambda_{\text{th}}}{1 + \sigma_{\tilde{w}}^2}\right)\right]. \end{aligned} \tag{3.17}$$

It is simple to see that the threshold that minimizes P_e is

$$\lambda_{\text{th}} = \sigma_{\tilde{w}}^2 (1 + \sigma_{\tilde{w}}^2) \ln\left(\frac{1 + \sigma_{\tilde{w}}^2}{\sigma_{\tilde{w}}^2}\right). \tag{3.18}$$

Now, using the above threshold for the general case (i.e., with multiuser interference), it is readily seen that

$$P\left(R_{n,m,l} \geq \lambda_{\text{th}} | K_{n,m,l}\right) = \exp\left(-\frac{\lambda_{\text{th}}}{K_{n,m,l} + \sigma_{\tilde{w}}^2}\right). \tag{3.19}$$

Obviously,

$$P\left(R_{n,m,l} \geq \lambda_{\text{th}} | K_{n,m,l} = 1\right) < P\left(R_{n,m,l} \geq \lambda_{\text{th}} | K_{n,m,l} > 1\right).$$

Thus, having two or more users transmitting in one chip time is more likely to yield a nonzero entry in $\mathbf{T}_n$. In general, there is an optimal threshold for each set of system parameters $M, K, L, \sigma_{\tilde{w}}^2$, which can be found by simulation [29]. However the sub-optimal threshold in (3.18) is more computation-friendly, while providing good performance. As such the threshold in (3.18) is also used in this chapter.

3.2.4 Receiver at the Destination

The general structure of the proposed receiver at the destination is shown in Fig. 3.5, which applies to both the AF and partial DF relaying schemes. Such a receiver makes use of the iterative (i.e., turbo) signal processing technique to handle the multi-user interference. The iteration is between the channel decoders and the interference cancellers.

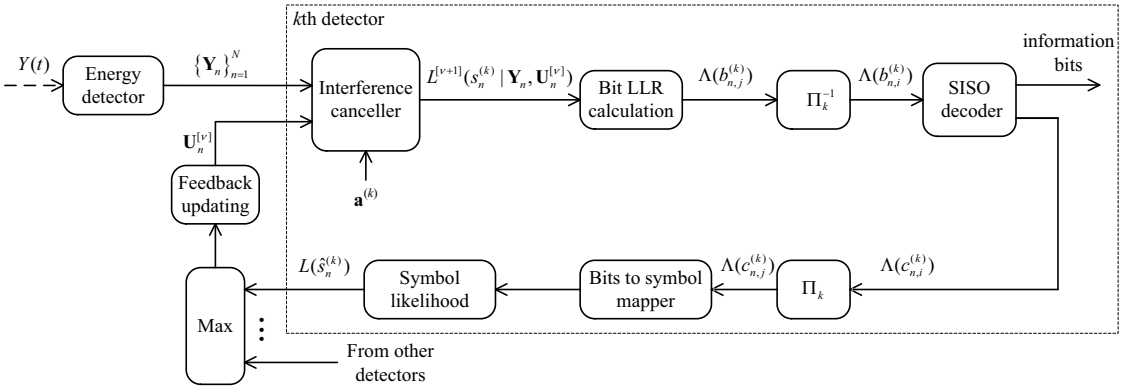

Figure 3.5 Structure of the receiver at the destination.

Let $Y(t)$ be the complex baseband-equivalent received signal at the destination over one frame duration, i.e., $0 \leq t \leq NT_s$. The front-end of the receiver first performs energy detection in the same way as what done in the relay (see Fig. 3.4) to obtain a set of normalized observation matrices $\mathcal{Y} = \{\mathbf{Y}_1, \mathbf{Y}_2, \ldots, \mathbf{Y}_N\}$. Next, the set $\mathcal{Y}$ is fed to a bank of K parallel detectors. Each detector is responsible for the decoding of one user. It is pointed out that the interference canceller tries to remove one interferer's signal after each iteration.

Therefore the maximum number of iterations is equal to number of concurrent users in the system. Without loss of generality, the main operations of the kth detector are described next.

In each iteration, the interference cancellation block carries out its computations on symbol-by-symbol basis. For the nth symbol duration, it makes use of the observation matrix $\mathbf{Y}_n$ together with the feedback information from the previous iteration to generate the probabilities (or likelihood values) for the nth symbol of the kth user. Let $\mathbf{U}_n^{[\nu]}$ be the $M \times L$ matrix that contains the feedback information from the νth iteration. Then the output of the kth interference canceller at the $(\nu+1)$th iteration is denoted by $P^{[\nu+1]}(s_n^{(k)}|\mathbf{Y}_n, \mathbf{U}_n^{[\nu]})$. Applying Bayes' theorem gives

$$P^{[\nu+1]}(s_n^{(k)}|\mathbf{Y}_n, \mathbf{U}_n^{[\nu]}) = \frac{p(\mathbf{Y}_n|s_n^{(k)}, \mathbf{U}_n^{[\nu]})P(s_n^{(k)})}{\sum_{\hat{s}=0}^{M-1} p(\mathbf{Y}_n|\hat{s}, \mathbf{U}_n^{[\nu]})P(\hat{s})}. \tag{3.20}$$

Under the assumption that all the entries of $\mathbf{Y}_n$ are independent random variables, one has

$$p(\mathbf{Y}_n|s_n^{(k)}, \mathbf{U}_n^{[\nu]}) = \prod_{m=0}^{M-1}\prod_{l=0}^{L-1} p(Y_{n,m,l}|s_n^{(k)}, U_{n,m,l}^{[\nu]}). \tag{3.21}$$

The computation of (3.21) depends on whether the AF or partial DF relaying is used. This computation is presented in detail in Section 3.3.

After each iteration of the whole receiver, the kth detector gives out N sets of *soft* likelihood values, one set having M values for each of the kth user's symbols. The feedback information is *updated* at the end of the νth iteration as follows. Over the nth symbol duration, the soft values of the $K-\nu+1$ users (i.e., detectors) who have not been decoded in any of the previous iterations are compared and the most likelihood symbol together with the user it belongs to are decided. That is, the additional feedback information over the nth symbol duration at the end of the νth iteration is of the form $\hat{s}_n^{(v_n)}$ for some user index v_n. The update of the information feedback matrix, $\mathbf{U}_n^{[\nu]}$, is

$$U_{n,m,l}^{[\nu]} = \begin{cases} U_{n,m,l}^{([\nu-1])} + 1, & \text{if } \hat{s}_n^{(v_n)} \oplus a_l^{(v_n)} = m \\ U_{n,m,l}^{([\nu-1])}, & \text{otherwise} \end{cases}. \tag{3.22}$$

Therefore, at the beginning of the $(\nu+1)$th iteration, individual locations of feedback matrix $\mathbf{U}_n^{[\nu]}$ take on values in the set $\{0, 1, \ldots, \nu-1\}$. The exact value gives valuable information

on how many users transmit over a specific time-frequency location. Such information is used by the interference canceller to refine the computation of the symbol likelihood values in the next iteration. It should also be noted that in the first iteration ($\nu = 1$), no feedback information is available, hence $\mathbf{U}_n^{[0]} = \mathbf{0}$.

The symbol likelihood values are then converted to the bit log-likelihood ratios (LLRs) so that they can be used by the SISO channel decoder. Let $b_{n,j}^{(k)}$ denote the bit at the jth position of symbol $s_n^{(k)}$. Considering the binary to M-ary mapping rule $b_{n,j}^{(k)} = (s_n^{(k)} 2^{-j}) \mod 2$, $j = 0, 1, \ldots, q-1$, one has

$$\begin{aligned} P(b_{n,j}^{(k)} = 0 | \mathbf{Y}_n, \mathbf{U}_n^{[\nu]}) &= \sum_{\hat{s}=0}^{M-1} \delta \left(\frac{\hat{s}}{2^j} \mod 2 \right) P(\hat{s} | \mathbf{Y}_n, \mathbf{U}_n^{[\nu]}) \\ &= \sum_{r=0}^{M/2-1} P\left(r + \left\lfloor \frac{r}{2^j} \right\rfloor 2^j \middle| \mathbf{Y}_n, \mathbf{U}_n^{[\nu]} \right), \end{aligned} \tag{3.23}$$

where $\lfloor \cdot \rfloor$ denotes the truncation function. Furthermore, the bit LLR can be written as

$$\Lambda(b_{n,j}^{(k)}) = \ln \left(\frac{P(b_{n,j}^{(k)} = 1 | \mathbf{Y}_n, \mathbf{U}_n^{[\nu]})}{P(b_{n,j}^{(k)} = 0 | \mathbf{Y}_n, \mathbf{U}_n^{[\nu]})} \right) = \ln \left(\frac{1 - P(b_{n,j}^{(k)} = 0 | \mathbf{Y}_n, \mathbf{U}_n^{[\nu]})}{P(b_{n,j}^{(k)} = 0 | \mathbf{Y}_n, \mathbf{U}_n^{[\nu]})} \right). \tag{3.24}$$

After being de-interleaved, $\Lambda(b_{n,j}^{(k)})$ becomes the *a priori* LLR, $\Lambda(b_{n,i}^{(k)})$, which can be used as the soft input for the SISO channel decoder. The decoder then computes the *a posteriori* LLR $\Lambda(c_{n,i}^{(k)})$ for each coded bit. That information is then interleaved and used to compute the log-likelihood values of the decoded symbol, $L(\hat{s}_n^{(k)})$. By the definition of $\Lambda(c_{n,i}^{(k)})$ and the mapping between $c_{n,j}^{(k)}$ and $\hat{s}_n^{(k)}$, one has

$$\begin{aligned} \Lambda(c_{n,j}^{(k)}) &= \ln \left(\frac{P(c_{n,j}^{(k)} = 1)}{P(c_{n,j}^{(k)} = 0)} \right) = \ln \left(\frac{P(c_{n,j}^{(k)} = 1)}{1 - P(c_{n,j}^{(k)} = 1)} \right) \\ &= \ln \left(\frac{P\left(c_{n,j}^{(k)} = \frac{\hat{s}_n^{(k)}}{2^j} \mod 2 \right)}{1 - P\left(c_{n,j}^{(k)} = \frac{\hat{s}_n^{(k)}}{2^j} \mod 2 \right)} \right), \quad j = 0, 1, \ldots, q-1. \end{aligned} \tag{3.25}$$

Under the assumption that the bits associated with a given symbol are independent, the log-likelihood values of a detected symbol can be computed from the LLR values of the coded

bits as

$$\begin{aligned} L(\hat{s}_n^{(k)}) &= \sum_{j=0}^{q-1} L(\hat{s}_n^{(k)}|c_{n,j}^{(k)}) = \sum_{j=0}^{q-1} L\left(c_{n,j}^{(k)} = \frac{\hat{s}_n^{(k)}}{2^j} \bmod 2\right) \\ &= \sum_{j=0}^{q-1} \left(\left|\Lambda(c_{n,j}^{(k)})\right| - \ln\left(1+\exp\left(\left|\Lambda(c_{n,j}^{(k)})\right|\right)\right)\right). \end{aligned} \tag{3.26}$$

The above outputs of the K detectors are used in the interference cancellers as follows. After each decoding stage, the output of one detector consists of N hard-decision symbols, $\hat{\mathbf{s}}^{(k)} = [\hat{s}_1^{(k)}, \hat{s}_2^{(k)}, \ldots, \hat{s}_N^{(k)}]$, together with their log-likelihood values $[L(\hat{s}_1^{(k)}), L(\hat{s}_2^{(k)}), \ldots, L(\hat{s}_N^{(k)})]$. The "Max" module compares these outputs from all the detectors to find one set of the N most reliable detected symbols as:

$$\hat{s}_n^{(v_n)} = \underset{v_n \in \mathbf{K}_n^{[\nu]}}{\operatorname{argmax}} \left\{L(\hat{s}_n^{(v_n)})\right\}, \quad n = 1, 2, \ldots, N, \tag{3.27}$$

where the maximization is over the set of users whose nth symbols have not been detected in the $(\nu-1)$ previous decoding stages, denoted as $\mathbf{K}_n^{[\nu]}$. The symbols $\{\hat{s}_n^{(v_n)}\}_{n=1}^N$ are then used to update matrix $\mathbf{U}_n^{[\nu]}$ as in (3.22), while the log-likelihood values $\{L(\hat{s}_n^{(v_n)})\}_{n=1}^N$ remain unchanged for the next iteration.

A simple example to illustrate how the proposed iterative receiver works is provided in Fig. 3.6 where the symbol likelihood values are shown. For this example, there are $K = 3$ users communicating to a destination using $M = 8$ frequency tones and $L = 4$ chip times. The frame length is taken to be $N = 5$, while the users' FH addresses are indicated in the figure. Focusing on the first symbol duration, given the numerical values provided in the figure, it can be readily seen that $\mathbf{K}_1^{[1]} = \{1, 2, 3\}$, $\mathbf{K}_1^{[2]} = \{1, 3\}$ and $\mathbf{K}_1^{[3]} = \{3\}$.

3.3 Interference Cancellation

This section examines in more detail the operation of the interference cancellation blocks in the iterative receiver. As pointed out before, the main task of this block is to compute (3.20), which is required in order to calculate $p(Y_{n,m,l}|s_n^{(k)}, U_{n,m,l}^{[\nu]})$ for (3.21).

Detector # \ Symbol #		1	2	3	4	5
1st iteration	$\hat{\mathbf{s}}^{(1)}$	6	2	2	7	5
	$L(\hat{\mathbf{s}}^{(1)})$	-0.6116	-1.2257	-0.0034	-0.6375	-0.5827
	$\hat{\mathbf{s}}^{(2)}$	4	5	5	7	1
	$L(\hat{\mathbf{s}}^{(2)})$	-0.0003	-1.0955	-0.2982	-0.4408	-0.0001
	$\hat{\mathbf{s}}^{(3)}$	7	3	2	6	2
	$L(\hat{\mathbf{s}}^{(3)})$	-0.2049	-0.0668	-0.0006	-0.5162	-0.0347
2nd iteration	$\hat{\mathbf{s}}^{(1)}$	2	2	2	5	5
	$L(\hat{\mathbf{s}}^{(1)})$	-0.0104	-0.2011	-0.0003	-0.3838	-0.5540
	$\hat{\mathbf{s}}^{(2)}$	4	3	0	7	1
	$L(\hat{\mathbf{s}}^{(2)})$	-0.0003	-0.5519	-0.0443	-0.0448	-0.0001
	$\hat{\mathbf{s}}^{(3)}$	7	3	2	7	0
	$L(\hat{\mathbf{s}}^{(3)})$	-0.0269	-0.0668	-0.0006	-0.0007	-0.5975
3rd iteration	$\hat{\mathbf{s}}^{(1)}$	2	2	2	5	5
	$L(\hat{\mathbf{s}}^{(1)})$	-0.0104	-0.2011	-0.0003	-0.0801	-0.5540
	$\hat{\mathbf{s}}^{(2)}$	4	7	0	7	1
	$L(\hat{\mathbf{s}}^{(2)})$	-0.0003	-0.206	-0.0007	-0.0448	-0.0001
	$\hat{\mathbf{s}}^{(3)}$	7	3	2	7	2
	$L(\hat{\mathbf{s}}^{(3)})$	-0.0021	-0.0668	-0.0006	-0.0007	-0.0047

Symbols decoded at 1st iteration
Symbols decoded at 2nd iteration
Symbols decoded at 3rd iteration
Symbols get fixed at later iteration

(a)

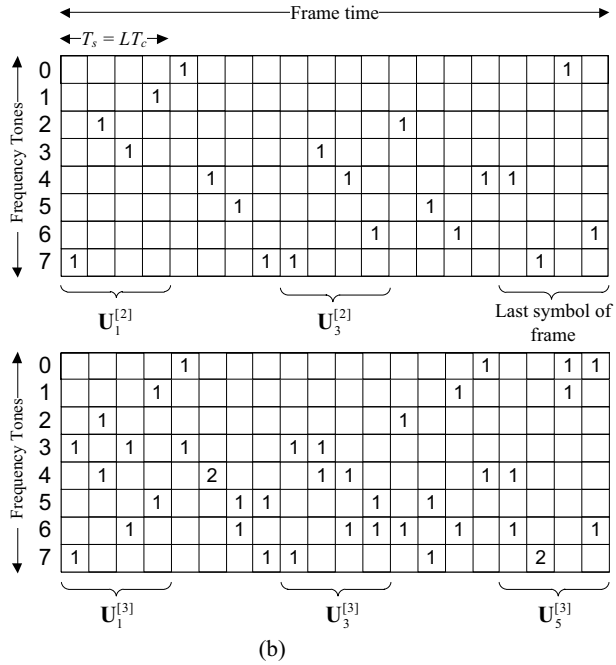

System Parameters
$M = 8$, $L = 4$, $K = 3$, $N = 5$
$\mathbf{a}^{(1)}$=[1,2,4,3]
$\mathbf{a}^{(2)}$=[3,6,7,5]
$\mathbf{a}^{(3)}$=[5,1,2,4]

(b)

Figure 3.6 Example illustrating the proposed iterative receiver: (a) Hard and soft outputs after each iteration, (b) Updating process of feedback matrix $\mathbf{U}_n^{[\nu]}$.

3.3.1 AF Relaying

When AF is used at the relay, the received complex baseband equivalent signal at the destination over the lth chip interval of nth symbol can be written as

$$Y_{n,l}(t) = \beta^{(\mathrm{AF})} g_{n,l} \tilde{R}_{n,l}(t) + \eta(t) = \beta^{(\mathrm{AF})} g_{n,l} \left(X_{n,l}(t) + \tilde{w}(t) \right) + \eta(t), \tag{3.28}$$

where the coefficient $g_{n,l} \sim \mathcal{CN}(0,1)$ represents the effect of the flat-fading channel between the relay and the destination and $\eta(t)$ is complex AWGN at the destination, whose one-sided power spectral density is N_0 per dimension. As in the MA phase, $g_{n,l}$'s are assumed to be independent over different chip durations [29].

With the above input signal, the normalized output of the energy detector can be computed as $Y_{n,m,l} = |y_{n,m,l}|^2$, where

$$\begin{aligned} y_{n,m,l} &= \frac{1}{T_c} \int_{lT_c+nT_s}^{(l+1)T_c+nT_s} \frac{Y_{n,l}(t)}{\beta^{(\mathrm{AF})}\sqrt{2E_c/T_c}} \psi(t - lT_c - nT_s) \exp(-j2\pi f_m t) \mathrm{d}t \\ &= g_{n,l} \left(\sum_{i=1}^{K} h_{n,l}^{(i)} \delta(f_{n,l}^{(i)} - f_m) + \tilde{w}_{n,m,l} \right) + \eta_{n,m,l}. \end{aligned} \tag{3.29}$$

In (3.29), the noise terms $\tilde{w}_{n,m,l}$ and $\eta_{n,m,l}$ are zero-mean circularly-symmetric complex Gaussian random variables with variances $\sigma_{\tilde{w}}^2 = N_0/E_c$ and $\sigma_\eta^2 = N_0/(\beta^{(\mathrm{AF})})^2 E_c$, respectively.

As shall be seen later, to calculate $p(Y_{n,m,l}|s_n^{(k)}, U_{n,m,l}^{[\nu]})$, it is useful to determine the distribution of $y_{n,m,l}$ given that there are k users who concurrently transmit with the same carrier frequency f_m during the time slot $lT_c + nT_s < t < (l+1)T_c + nT_s$. Denote this distribution as $p(y_{n,m,l}|k)$. Given k, the first term in (3.29), namely $x_{n,m,l} = \left(\sum_{i=1}^{K} h_{n,l}^{(i)} \delta(f_{n,l}^{(i)} - f_m) + \tilde{w}_{n,m,l} \right)$, is a complex Gaussian random variable of zero-mean and variance $\sigma_x^2 = k + \sigma_{\tilde{w}}^2$. Using the distribution of a product of two independent complex Gaussian random variables in [53], the pdf of $y_{n,m,l}$ conditioned on k and $\eta_{n,m,l}$ is

$$p(y_{n,m,l}|k, \eta_{n,m,l}) = \frac{2}{\pi(k + \sigma_{\tilde{w}}^2)} K_0 \left(\frac{2|y_{n,m,l} - \eta_{n,m,l}|}{\sqrt{k + \sigma_{\tilde{w}}^2}} \right), \tag{3.30}$$

where $K_0(\cdot)$ is the zero-order modified Bessel function of the second kind.

In order to obtain $p(y_{n,m,l}|k)$, one has to take the expectation of (3.30) over $\eta_{n,m,l}$. Unfortunately, there is no closed-form expression for such expectation. To overcome this difficulty,

the following approximation, similar to what used in [53], is proposed:

$$p(y_{n,m,l}|k) \sim \frac{2}{\pi(k+\sigma_{\tilde{w}}^2)} K_0\left(\frac{2}{\sqrt{k+\sigma_{\tilde{w}}^2}}\sqrt{|y_{n,m,l}|^2+\sigma_\eta^2}\right). \tag{3.31}$$

Correspondingly, the following approximation is used for $p(Y_{n,m,l}|k)$:

$$p(Y_{n,m,l}|k) \sim \frac{2}{\pi(k+\sigma_{\tilde{w}}^2)} K_0\left(\frac{2}{\sqrt{k+\sigma_{\tilde{w}}^2}}\sqrt{Y_{n,m,l}+\sigma_\eta^2}\right). \tag{3.32}$$

Next, the pdf $p(Y_{n,m,l}|s_n^{(k)}, U_{n,m,l}^{[\nu]})$ is calculated as follows:

$$\begin{aligned} p(Y_{n,m,l}|s_n^{(k)}, U_{n,m,l}^{[\nu]}) = {} & p(Y_{n,m,l}|U_{n,m,l}^{[\nu]}, S_{n,m,l}^{(k)}=1)\cdot P(S_{n,m,l}^{(k)}=1|s_n^{(k)}) \\ & + p(Y_{n,m,l}|U_{n,m,l}^{[\nu]}, S_{n,m,l}^{(k)}=0)\cdot P(S_{n,m,l}^{(k)}=0|s_n^{(k)}). \end{aligned} \tag{3.33}$$

Since all the K users transmit their signals simultaneously in the MA phase, there exists interference from a number of users at each chip time. At the νth iteration, there are $(\nu-1)$ symbols decoded over each symbol duration that are determined for $(\nu-1)$ users in the previous iterations. The symbol information from other $(K-\nu)$ users remains unknown and should be treated as interference. After each iteration, one more symbol is decoded and the number of interferers reduces by one. Specifically, the distribution of $Y_{n,m,l}$ at a single TF location depends on three factors: (i) the transmitted symbol $s_n^{(k)}$, (ii) the $\nu-1$ decoded symbols from previous iterations, which can be seen from $U_{n,m,l}^{[\nu-1]}$, and (iii) the random interference from the remaining $K-\nu$ users.

Let J, $0 \le J \le (K-\nu)$, be the number of interferers in one particular TF location. Then one has

$$p(Y_{n,m,l}|U_{n,m,l}^{[\nu]}, S_{n,m,l}^{(k)}=1) = \sum_{j=0}^{K-\nu} p(Y_{n,m,l}|U_{n,m,l}^{[\nu]}, S_{n,m,l}^{(k)}=1, J=j)P(J=j). \tag{3.34}$$

As pointed out before, the probability $P(J=j)$ is determined by the binomial distribution $B(K-\nu, j, 1/M)$. On the other hand, $p(Y_{n,m,l}|U_{n,m,l}^{[\nu]}, S_{n,m,l}^{(k)}=1, J=j)$ is concerned with the distribution of the energy measured at the (n,m,l) TF location under the hypothesis that there are $U_{n,m,l}^{[\nu]}$ decoded users (coming from the feedback information), one user of interest

and j interferers who are active in that TF location. It then follows from (3.32) that

$$p(Y_{n,m,l}|U^{[\nu]}_{n,m,l}, S^{(k)}_{n,m,l}=1, J=j) = \frac{2}{\pi(U^{[\nu]}_{n,m,l}+1+j+\sigma^2_{\tilde{w}})} K_0\left(2\sqrt{\frac{Y_{n,m,l}+\sigma^2_\eta}{(U^{[\nu]}_{n,m,l}+1+j+\sigma^2_{\tilde{w}})}}\right). \tag{3.35}$$

Substituting (3.35) into (3.34) yields

$$p(Y_{n,m,l}|U^{[\nu]}_{n,m,l}, S^{(k)}_{n,m,l}=1) = \sum_{j=0}^{K-\nu} \frac{2B(K-\nu,j,1/M)}{\pi(U^{[\nu]}_{n,m,l}+1+j+\sigma^2_{\tilde{w}})} K_0\left(2\sqrt{\frac{Y_{n,m,l}+\sigma^2_\eta}{(U^{[\nu]}_{n,m,l}+1+j+\sigma^2_{\tilde{w}})}}\right). \tag{3.36}$$

Similarly, one has

$$p(Y_{n,m,l}|U^{[\nu]}_{n,m,l}, S^{(k)}_{n,m,l}=0) = \sum_{j=0}^{K-\nu} \frac{2B(K-\nu,j,1/M)}{\pi(U^{[\nu]}_{n,m,l}+j+\sigma^2_{\tilde{w}})} K_0\left(2\sqrt{\frac{Y_{n,m,l}+\sigma^2_\eta}{(U^{[\nu]}_{n,m,l}+j+\sigma^2_{\tilde{w}})}}\right). \tag{3.37}$$

Then substituting the two above equations into (3.33) gives

$$\begin{aligned} p(Y_{n,m,l}|s^{(k)}_n, U^{[\nu]}_{n,m,l}) = & \\ & P(S^{(k)}_{n,m,l}=1|s^{(k)}_n) \cdot \sum_{j=0}^{K-\nu} \frac{2B(K-\nu,j,1/M)}{\pi(U^{[\nu]}_{n,m,l}+1+j+\sigma^2_{\tilde{w}})} K_0\left(2\sqrt{\frac{Y_{n,m,l}+\sigma^2_\eta}{(U^{[\nu]}_{n,m,l}+1+J+\sigma^2_{\tilde{w}})}}\right) \\ & + P(S^{(k)}_{n,m,l}=0|s^{(k)}_n) \cdot \sum_{j=0}^{K-\nu} \frac{2B(K-\nu,j,1/M)}{\pi(U^{[\nu]}_{n,m,l}+j+\sigma^2_{\tilde{w}})} K_0\left(2\sqrt{\frac{Y_{n,m,l}+\sigma^2_\eta}{(U^{[\nu]}_{n,m,l}+j+\sigma^2_{\tilde{w}})}}\right). \end{aligned} \tag{3.38}$$

In the above expression, the quantity $P(S^{(k)}_{n,m,l}=1|s^{(k)}_n) = 1 - P(S^{(k)}_{n,m,l}=0|s^{(k)}_n)$ is determined by the M-FSK mapping rule. It takes on a value of 1 or 0 depending on the FH address $\mathbf{a}^{(k)}$ of the kth user and the transmitted symbol $s^{(k)}_n$.

It should also be pointed out that, although the AF is a simple operation at the relay, the computing of $p(Y_{n,m,l}|s^{(k)}_n, U^{[\nu]}_{n,m,l})$ in (3.38) is quite complicated due to the presence of the modified Bessel function. In practical implementation, one would pre-compute the modified Bessel function for a large set of its argument, store the values in the read-only memory (ROM) and use them to approximate the true values.

3.3.2 Partial DF Relaying

For the case of partial DF relaying, the received complex baseband-equivalent signal at the destination is given as

$$Y(t) = \beta^{(\mathrm{DF})}\sqrt{\frac{2E_c}{T_c}}\sum_{n=0}^{N-1}\sum_{l=0}^{L-1} g_{n,l}\left(\sum_{m=0}^{M-1}\delta(T_{n,m,l}-1)\psi(t-lT_c-nT_s)\exp\left(j2\pi f_m t\right)\right)+\eta(t),$$
$$0 \le t \le NT_s. \quad (3.39)$$

The normalized output of the energy detector is

$$\begin{aligned} Y_{n,m,l} &= \left|\frac{1}{T_c}\int_{lT_c+nT_s}^{(l+1)T_c+nT_s}\frac{Y(t)}{\beta^{(\mathrm{DF})}\sqrt{2E_c/T_c}}\psi(t-lT_c-nT_s)\exp(-j2\pi f_m t)\mathrm{d}t\right|^2 \\ &= \left|g_{n,l}\cdot\delta(T_{n,m,l}-1)+\eta_{n,m,l}\right|^2. \end{aligned} \quad (3.40)$$

As in the AF relaying case, the noise term $\eta_{n,m,l}$ is a zero-mean circularly-symmetric complex Gaussian random variable with variance $\sigma_\eta^2 = N_0/(\beta^{(\mathrm{DF})})^2E_c$. It can be seen that $Y_{n,m,l}$ is an exponential variable, whose mean value is either $(1+\sigma_\eta^2)$ if its location corresponds to a nonzero signal transmitted by the relay, or σ_η^2 otherwise.

Finding the expression of $p(Y_{n,m,l}|s_n^{(k)}, U_{n,m,l}^{[\nu]})$ can be done by taking into account the decision made at the relay. Specifically, one has

$$\begin{aligned} p(Y_{n,m,l}|s_n^{(k)}, U_{n,m,l}^{[\nu]}) &= p(Y_{n,m,l}|T_{n,m,l}=1)\cdot P(T_{n,m,l}=1|s_n^{(k)}, U_{n,m,l}^{[\nu]}) \\ &\quad + p(Y_{n,m,l}|T_{n,m,l}=0)\cdot P(T_{n,m,l}=0|s_n^{(k)}, U_{n,m,l}^{[\nu]}). \end{aligned} \quad (3.41)$$

It follows from (3.40) that

$$p(Y_{n,m,l}|T_{n,m,l}=1) = \frac{1}{1+\sigma_\eta^2}\exp\left(-\frac{Y_{n,m,l}}{1+\sigma_\eta^2}\right), \quad (3.42)$$

and

$$p(Y_{n,m,l}|T_{n,m,l}=0) = \frac{1}{\sigma_\eta^2}\exp\left(-\frac{Y_{n,m,l}}{\sigma_\eta^2}\right). \quad (3.43)$$

On the other hand, since $\mathbf{T}_n$ is obtained by comparing the entries of $\mathbf{R}_n$ with threshold λ_{th} as in (3.11), one has

$$P(T_{n,m,l}=0|s_n^{(k)}, U_{n,m,l}^{[\nu]}) = 1-P(T_{n,m,l}=1|s_n^{(k)}, U_{n,m,l}^{[\nu]}) = P(R_{n,m,l}<\lambda_{\mathrm{th}}|s_n^{(k)}, U_{n,m,l}^{[\nu]}). \quad (3.44)$$

To determine the probability $P(R_{n,m,l} < \lambda_{\text{th}} | s_n^{(k)}, U_{n,m,l}^{[\nu]})$, the conditional pdf of $R_{n,m,l}$ is needed. It is computed as follows:

$$p(R_{n,m,l}|s_n^{(k)}, U_{n,m,l}^{[\nu]}) = p(R_{n,m,l}|U_{n,m,l}^{[\nu]}, S_{n,m,l}^{(k)} = 1) \cdot P(S_{n,m,l}^{(k)} = 1|s_n^{(k)}) + p(R_{n,m,l}|U_{n,m,l}^{[\nu]}, S_{n,m,l}^{(k)} = 0) \cdot P(S_{n,m,l}^{(k)} = 0|s_n^{(k)}), \quad (3.45)$$

where, similar to the expression in (3.38) for the case of AF relaying, the two probabilities $P(S_{n,m,l}^{(k)} = 1|s_n^{(k)})$ and $P(S_{n,m,l}^{(k)} = 0|s_n^{(k)})$ take on a value of 1 or 0 depending on the FH address $\mathbf{a}^{(k)}$ of the kth user and the transmitted symbol $s_n^{(k)}$. Also, similar to the calculation of $p(Y_{n,m,l}|U_{n,m,l}^{[\nu]}, S_{n,m,l}^{(k)} = 1)$ in (3.34), the conditional densities $p(R_{n,m,l}|U_{n,m,l}^{[\nu]}, S_{n,m,l}^{(k)} = 1)$ and $p(R_{n,m,l}|U_{n,m,l}^{[\nu]}, S_{n,m,l}^{(k)} = 0)$ can be found by considering the number of unknown interferers at the νth iteration, which can take any value between 0 and $(K - \nu)$. Specifically,

$$\begin{aligned} p(R_{n,m,l}|U_{n,m,l}^{[\nu]}, S_{n,m,l}^{(k)} = 1) &= \sum_{j=0}^{K-\nu} p(R_{n,m,l}|U_{n,m,l}^{[\nu]}, S_{n,m,l}^{(k)} = 1, J = j) \cdot P(J = j) \\ &= \sum_{j=0}^{K-\nu} \frac{B(K-\nu, j, 1/M)}{U_{n,m,l}^{[\nu]} + 1 + j + \sigma_{\tilde{w}}^2} \exp\left(-\frac{R_{n,m,l}}{U_{n,m,l}^{[\nu]} + 1 + j + \sigma_{\tilde{w}}^2}\right), \end{aligned} \quad (3.46)$$

and

$$p(R_{n,m,l}|U_{n,m,l}^{[\nu]}, S_{n,m,l}^{(k)} = 0) = \sum_{j=0}^{K-\nu} \frac{B(K-\nu, j, 1/M)}{U_{n,m,l}^{[\nu]} + j + \sigma_{\tilde{w}}^2} \exp\left(-\frac{R_{n,m,l}}{U_{n,m,l}^{[\nu]} + j + \sigma_{\tilde{w}}^2}\right). \quad (3.47)$$

Finally, by substituting (3.47) and (3.46) into (3.45) and performing integration, one obtains:

$$\begin{aligned} &P(T_{n,m,l} = 0|s_n^{(k)}, U_{n,m,l}^{[\nu]}) = \\ &\quad P(S_{n,m,l}^{(k)} = 1|s_n^{(k)}) \sum_{j=0}^{K-\nu} \frac{B(K-\nu, j, 1/M)}{U_{n,m,l}^{[\nu]} + 1 + j + \sigma_{\tilde{w}}^2} \int_0^{\lambda_{\text{th}}} \exp\left(\frac{-x}{U_{n,m,l}^{[\nu]} + 1 + j + \sigma_{\tilde{w}}^2}\right) \mathrm{d}x \\ &\quad + \left(1 - P(S_{n,m,l}^{(k)} = 1|s_n^{(k)})\right) \sum_{j=0}^{K-\nu} \frac{B(K-\nu, j, 1/M)}{U_{n,m,l}^{[\nu]} + j + \sigma_{\tilde{w}}^2} \int_0^{\lambda_{\text{th}}} \exp\left(\frac{-x}{U_{n,m,l}^{[\nu]} + j + \sigma_{\tilde{w}}^2}\right) \mathrm{d}x \\ &\quad = \sum_{j=0}^{K-\nu} B(K-\nu, j, 1/M) \left(1 - \exp\left(\frac{-\lambda_{\text{th}}}{U_{n,m,l}^{[\nu]} + j + \sigma_{\tilde{w}}^2}\right)\right) + P(S_{n,m,l}^{(k)} = 1|s_n^{(k)}) \times \\ &\sum_{j=0}^{K-\nu} B(K-\nu, j, 1/M) \left(\exp\left(\frac{-\lambda_{\text{th}}}{U_{n,m,l}^{[\nu]} + j + \sigma_{\tilde{w}}^2}\right) - \exp\left(\frac{-\lambda_{\text{th}}}{U_{n,m,l}^{[\nu]} + 1 + j + \sigma_{\tilde{w}}^2}\right)\right). \end{aligned} \quad (3.48)$$

It should be pointed out that, for fixed parameters $M, K, \lambda_{\text{th}}$, the above probability can be computed once at the beginning of each iteration. Moreover, since $P(S_{n,m,l}^{(k)} = 1|s_n^{(k)})$ is 0 or 1 and $U_{n,m,l}^{[\nu]}$ takes on integer values ranging from 0 to $(\nu - 1)$, at the νth iteration one can pre-compute and store 2ν quantities instead of repeating the calculation for every (m, l) location.

To avoid the numerical instability issue in implementation, instead of computing the probability values $P(s_n^{(k)}|\mathbf{Y}_n, \mathbf{U}_n^{[\nu]})$, it is possible to perform all the related calculations in the log-domain and compute the L-values $L(s_n^{(k)}|\mathbf{Y}_n, \mathbf{U}_n^{[\nu]}) = \ln P(s_n^{(k)}|\mathbf{Y}_n, \mathbf{U}_n^{[\nu]})$. The details are given in Appendix A.

3.4 Simulation Results

This section presents the simulation results of the bit-error-rate (BER) performance of the proposed multiuser relaying system. All simulations are done in MATLAB. First, a constraint-length 7, rate$-1/2$ convolutional code with generator polynomials $\mathbf{g}^{(0)} = [2, 4, 7]$ and $\mathbf{g}^{(1)} = [3, 7, 1]$ (in octal form) is employed. This is the best convolutional code for given constraint length and code rate and its free Euclidean distance is $d_{\text{free}} = 10$ [54]. The information block length is set to be 1920 bits. Thus, for a system with $M = 16$ or $M = 32$ frequency tones, one code block contains 480 or 384 M-FSK symbols, respectively. Each user is assigned a different S-random interleaver with the spreading factor of 25. The power allocated for the relay is set to be $P_{\text{tx}}^{(\text{R})} = KP_{\text{tx}}^{(k)}$. This setup results in the same average SNR in all transmission links, i.e., from users to relay, and from relay to destination. The SNR shown in all figures of this section is the average SNR per information bit, given as in (3.4). On the other hand, given similar channel conditions experienced by each user, all users are expected to have similar BER performance and the BER curves plotted in all figures are averaged over all users.[1] Also note that since the use of coding reduces the transmission rate, in order to have a fair comparison (in terms of spectral efficiency) with the uncoded transmission in [29], our system only uses half the number of chip times that would be used in the uncoded system. The spectral efficiency is measured as $\mu = \frac{R_c K \log_2(M)}{LM}$ (bit/s/Hz).

[1]When plotted separately, the BER curves of individual users essentially overlap each other.

First, the performance of the AF relaying system is shown in Fig. 3.7 for system parameters of $M = 16$, $K = 5$ and $L = 4$. It can be seen that remarkable performance improvements with iterations of the proposed receiver are achieved. Moreover, the proposed system (with channel coding) is able to provide a huge performance boost over the uncoded system (which uses $L = 8$) that employs the maximum-likelihood multiuser detection (MUD) as studied in [29].

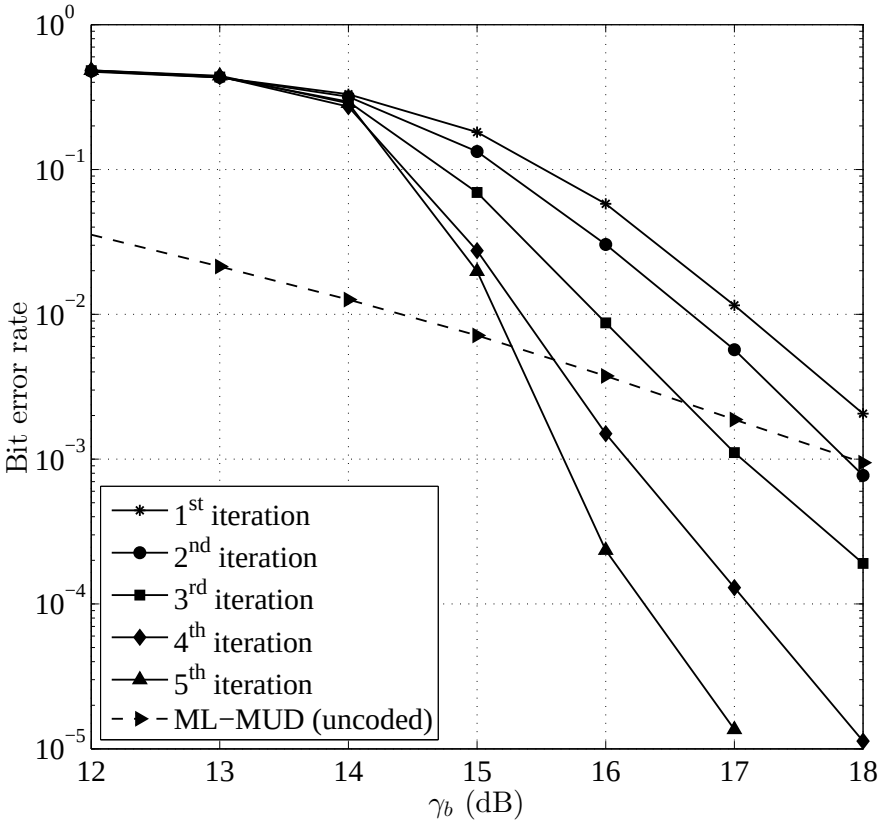

Figure 3.7 BER performance of the AF relaying system with $M = 16$.

Of particular interest is the performance of the proposed partial DF relaying system, which is shown in Fig. 3.8 for a system configured with $M = 16$, $K = 5$ and $L = 4$, and in Fig. 3.9 for a system with $M = 32$, $K = 6$ and $L = 3$. Note that the spectral efficiency of these two systems is $\mu = 0.1563$ (bit/s/Hz). Compared to Fig. 3.7, Fig. 3.8 clearly shows that the proposed partial DF relaying outperforms the AF relaying. At the last stage of decoding, the proposed partial DF relaying achieves a coding gain of 3.5dB[2] (measured at

[2]As 3dB means two times in linear scale, a 3.5dB of coding gain can help to reduce the transmitted power

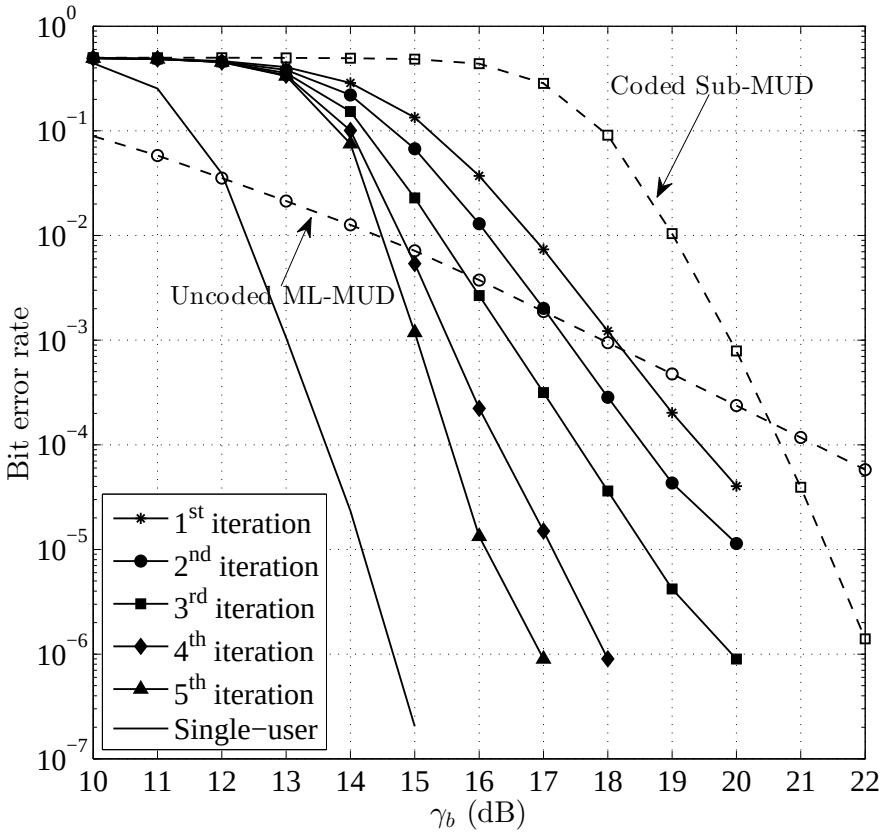

Figure 3.8 BER performance of the proposed partial DF relaying system with $M = 16$.

the BER level of 10^{-4}) when compared to the performance of the first-state decoding (i.e., decoding with no feedback for interference cancellation) and 6.5dB better than the uncoded system using the optimal ML-MUD. However, there is about 2dB gap when compared to the single-user performance (i.e., when there is no interference).

Also included for comparison in Fig. 3.8 is the BER of a partial DF system with channel coding, but instead of the proposed iterative receiver, the destination employs a suboptimal-MUD (Sub-MUD) [29], which feeds hard decisions to the K channel decoders. It is pointed out that, although the complexity of the Sub-MUD is significant lower than that of the ML-MUD, detection with Sub-MUD still involves searching multi-user symbols, whose complexity grows quickly with the number of users. As can be seen from Fig. 3.8, such a coded partial

by about 55 percent.

DF system (which uses $L = 4$ and rate$-1/2$ convolutional code) outperforms the uncoded partial DF system (which uses the ML-MUD) only in a fairly high SNR region (> 20 dB), but its performance is significantly inferior to the performance of the proposed iterative receiver for the whole range of SNR.

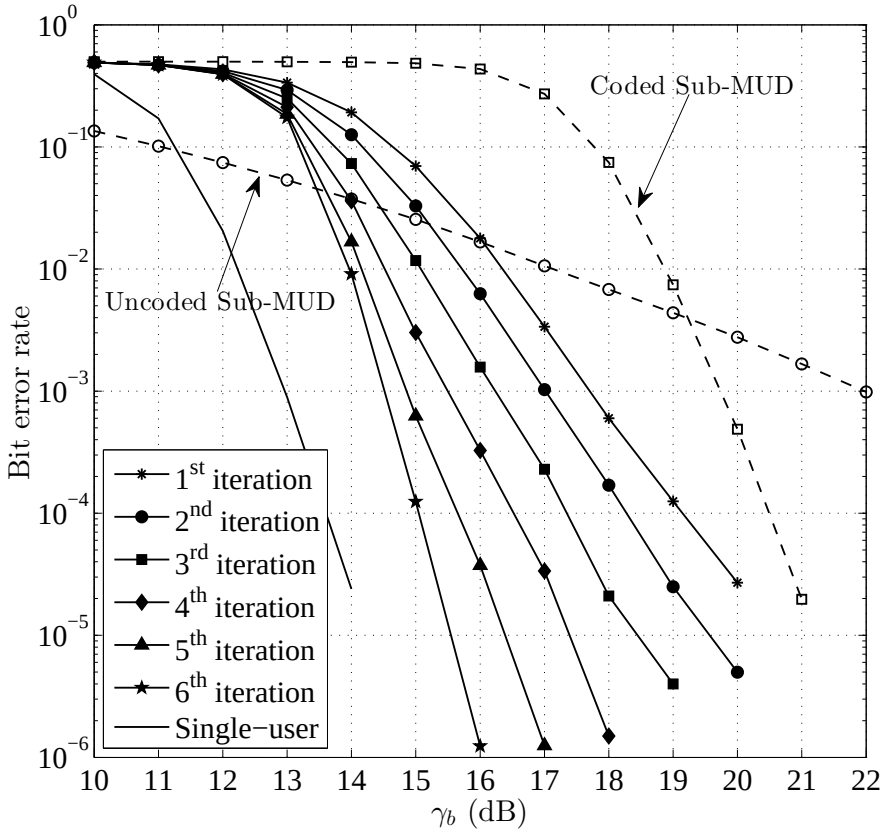

Figure 3.9 BER performance of the proposed partial DF relaying system with $M = 32$.

Similar observations hold for Fig. 3.9. For example, assuming that the target BER level is 10^{-4}, the performance at the last iteration delivers a coding gain of 4dB over the performance at the first iteration, and less than 2dB away from the performance of a single-user system. It is pointed out that the optimal ML-MUD is simply not possible for the considered system parameters. Instead the suboptimal MUD (Sub-MUD) is used. The proposed system is able to provide a performance boost of about 11dB over the uncoded system (which uses $L = 6$) that employs a Sub-MUD proposed in [29]. Likewise, there is about 5.5dB SNR gain achieved by the proposed system over a coded system whose destination uses the Sub-MUD

and hard-input Viterbi decoding without successive interference cancellation.

Finally, Fig. 3.10 illustrates the ability of the proposed partial DF relaying system in supporting multiple users under various system setups. In particular, shown in the figure are the BER curves versus the number of users when the spectral efficiency is maintained at $\mu = 0.1563$ (bit/s/Hz), while different combinations of number of time slots and code rate are investigated. The other system parameters are $M = 32$ and $\gamma_b = 20$ dB and all codes are the best codes (in terms of maximizing the free Euclidean distance) of constraint length 7 [54, 55]. It can be seen that, for a given BER requirement, using a higher code rate can help to support more users. For example, at the BER requirement of 10^{-4}, 5 more users can be supported by using rate-5/6 code instead of rate-1/3 code. The main reason for this phenomenon is that in order to maintain a given spectral efficiency, using a low-rate code requires a smaller number of chip times, which means that it is more difficult to resolve interference ambiguity when the number of user increases. It should be noted, however, that a higher-rate code is more complicated to decode with the SISO algorithm. In general, there should be an optimal combination of code rate, number of chip times, and number of sub-carriers to maximize the system throughput; finding such an optimal combination deserves further research.

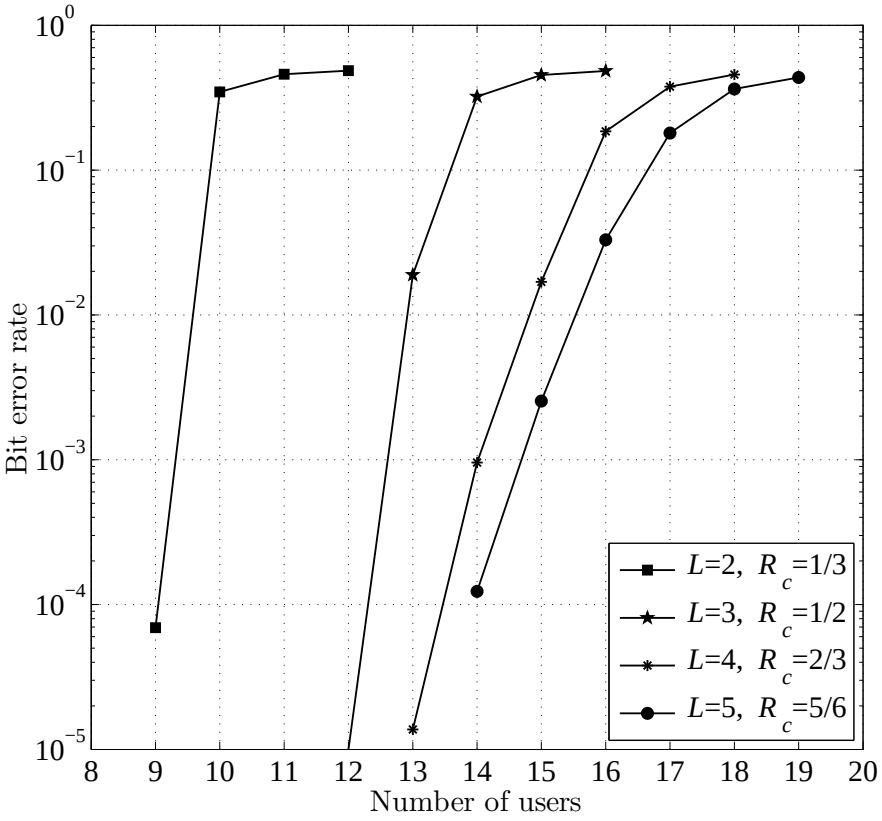

Figure 3.10 Overall BER versus the number of users for the proposed partial DF relaying system with $M = 32$ and $\gamma_b = 20$ dB.

4. Improved Receiver with Inner-Loop Iterations

4.1 Introduction

The structure of the receiver proposed in this chapter is slightly more complex than the one presented in the previous chapter, where the symbol-to-bit LLR calculation module is replaced with the soft demapper block. With the proposed IIC algorithm in Chapter 3 that already employs a SISO decoder, it is convenient to further exploit the SISO decoder's soft output to perform an update on the output statistics of the soft demapper. By doing so, the inner-loop process resembles a receiver in a bit-interleaved coded modulation with iterative decoding (BICM-ID) system. The structure of a BICM-ID system is shown in Fig. 4.1.

The technique of bit-interleaved coded modulation (BICM) was first introduced by Zehavi [56] in 1992 as an effective method to improve the performance of a coded modulation system over a fading channel. With BICM, binary information bits are encoded then bit-wised interleaved before passing to an M-ary mapper/modulator. In a conventional BICM receiver, a soft demapper produces soft estimations of coded bits then passes them to a soft-input decoder [57]. In comparison to the more classical trellis coded modulation (TCM) approach of Ungerboeck [58], performance of BICM system is slightly inferior in an AWGN channel where the Euclidean distance is the primary factor determining the error rate. However, the real advantage of BICM is realized in a fading channel because it maximizes the Hamming distance between any two transmitted sequences. The Hamming distance is more important than the Euclidean distance when considering the effect of fading.

Inspired by the invention of turbo codes and iterative (turbo) decoding, ten Brink *et al.* [59] showed that the performance of a BICM system can be significantly improved by

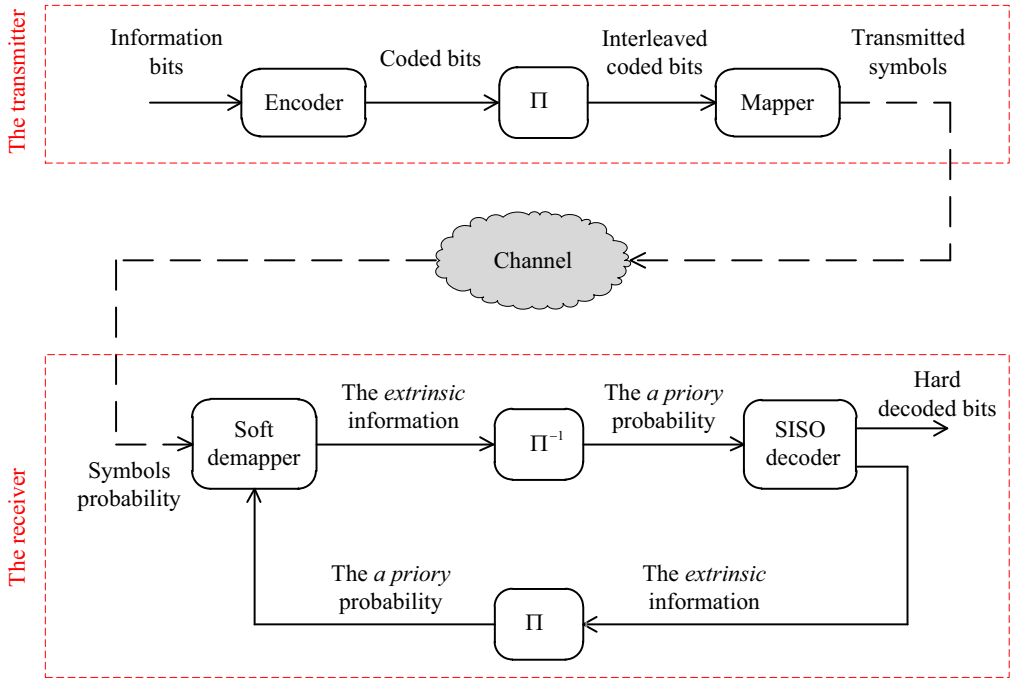

Figure 4.1 Transmitter and receiver of a BICM-ID system.

iteratively feeding back the soft information from the SISO channel decoder to the soft demapper. This method regards mapper as an *outer* binary rate-1 block encoder which is serially concatenated with the channel encoder (which plays the role of an *inner* encoder) through an interleaver. In this way the principle of turbo decoding can be effectively applied. The framework of BICM-ID has been investigated extensively and applied to many different communication systems in the last decade [60]. It is pointed out that BICM-ID has also been successfully applied to other modulation formats that are suitable for non-coherent or differentially-coherent detection, such as differential phase shift keying (DPSK) [61].

4.2 Structure of the Two-Loop Receiver

The structure of the proposed two-loop receiver is illustrated in Fig. 4.2. Compared to the receiver in Chapter 3, the major modifications are made inside the "Inner loop" block, in which the symbol likelihood $P^{[\nu+1]}(s_n^{(k)}|\mathbf{Y}_n, \mathbf{U}_n^{[\nu]})$ is processed to give out decoded information bits as well as the soft-output of each coded bit in the form of the *a posteriori*

LLR, denoted as $\Lambda^O(c_{n,i}^{(k)})$. By subtracting the *a priori* LLR, $\Lambda^I(b_{n,i}^{(k)})$, from the *a posteriori* LLR, the *extrinsic* LLR, $\Lambda^O(x_{n,i}^{(k)})$, can be obtained. The content of the extrinsic LLR is independent on coded information and only influenced by the structure of the code itself, hence the name "extrinsic". After interleaving, the extrinsic LLR becomes the *a priori* LLR, $\Lambda^I(x_{n,j}^{(k)})$, to the soft demapper.

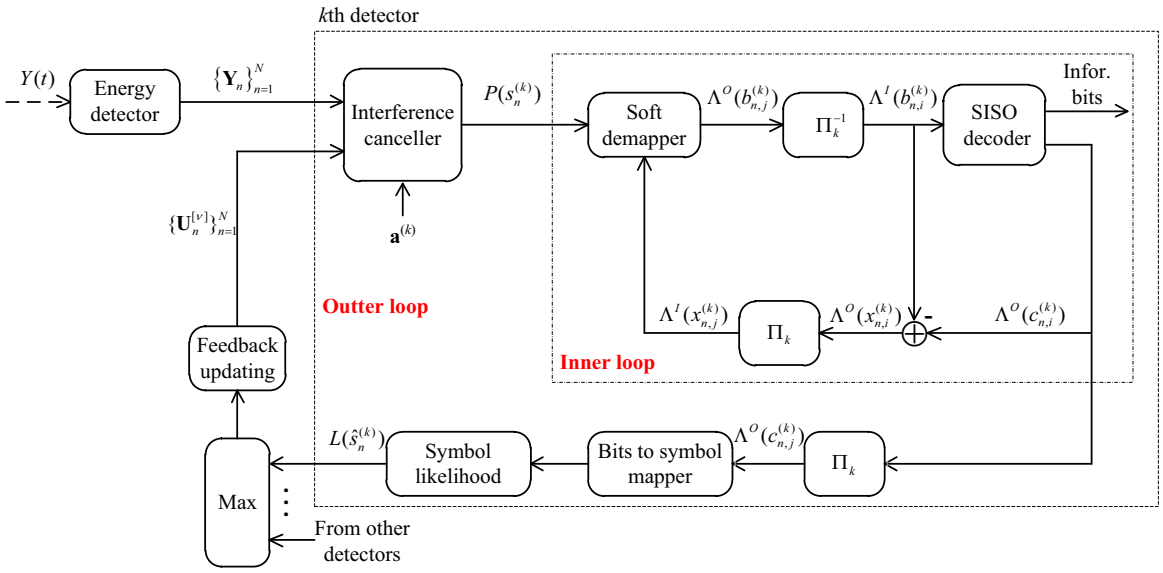

Figure 4.2 Structure of the two-loop receiver.

Interestingly, since the bit-to-symbol mapper module can be considered as a rate-1 convolutional encoder, the soft demapper can be realized as a rate-1 SISO decoder that generates soft estimations on the coded bits. Therefore, one can employ trellis-based soft-output decoding algorithms to deliver additional reliability information together with hard decisions [54]. In terms of maximizing the *a posteriori* probability (MAP) of the symbol sequence (that belongs to one frame), the Viterbi decoder [62] is known as the optimum decoder because it gives a solution to the problem of MAP estimation of the state sequence of a finite-state discrete-time Markov process. While that ML decoding method minimizes the frame (or sequence) error rate, it does not necessarily minimize the probability of bit error. In fact, the Bahl-Cocke-Jelinek-Raviv (BCJR) algorithm [63] (also known as the symbol-by-symbol MAP algorithm or MAP algorithm for short) is considered optimum in terms of minimizing

the bit error rate.

The soft demapper is implemented based on the MAP algorithm which has been generally described in [64]. Specifically, the soft demapper takes as its inputs the likelihood $P(s_n^{(k)}) = \left\{ P^{[\nu+1]}(s_n^{(k)} = \hat{s} | \mathbf{Y}_n, \mathbf{U}_n^{[\nu]}), \hat{s} = 0, 1, \ldots, M-1 \right\}$ and probability distribution functions $p(x_{n,j}^{(k)}; I) = \left\{ p(x_{n,j}^{(k)} = \alpha; I),\ \alpha \in \{0,1\} \right\},\ j = 0, 1, \ldots, q-1$ and generates output distributions $p(b_{n,j}^{(k)}; O) = \left\{ p(b_{n,j}^{(k)} = \alpha; O),\ \alpha \in \{0,1\} \right\},\ j = 0, 1, \ldots, q-1$. Since the operation of the inner-loop iteration can be explained on a symbol-by-symbol basis, the appearance of matrices $\mathbf{Y}$ and $\mathbf{U}$ as well as the superscript $[\nu]$ (that denotes the iteration number) can be dropped without raising any ambiguity. That is, the expression in (3.20) is simplified to $P(s_n^{(k)}) \equiv P^{[\nu+1]}(s_n^{(k)} | \mathbf{Y}_n, \mathbf{U}_n^{[\nu]})$. Moreover, the distributions $p(x_{n,j}^{(k)}; I)$ can be related to the *extrinsic* likelihood ratios as

$$\frac{p(x_{n,j}^{(k)} = 1; I)}{p(x_{n,j}^{(k)} = 0; I)} = \frac{P(x_{n,j}^{(k)} = 1)}{P(x_{n,j}^{(k)} = 0)} = \exp\left(\Lambda^I(x_{n,j}^{(k)}) \right). \tag{4.1}$$

It then follows that the input distributions of the soft demapper can be effectively calculated from the *extrinsic* LLR as

$$p(x_{n,j}^{(k)} = \alpha; I) = \frac{\exp\left(\Lambda^I(x_{n,j}^{(k)}) \cdot \alpha \right)}{1 + \exp\left(\Lambda^I(x_{n,j}^{(k)}) \right)}, \quad \alpha = 0, 1. \tag{4.2}$$

Likewise, the output distribution functions $p(b_{n,j}^{(k)}; O)$ can be conveniently written as the LLR as

$$\Lambda^O(b_{n,j}^{(k)}) = \frac{p(b_{n,j}^{(k)} = 1; O)}{p(b_{n,j}^{(k)} = 0; O)}. \tag{4.3}$$

Next, consider the bit-to-symbol mapping rule in (3.23). Let $\mathcal{S}_j^{(0)} = \left\{ r + \left\lfloor \frac{r}{2^j} \right\rfloor 2^j \right\}_{r=0}^{M/2-1}$ and $\mathcal{S}_j^{(1)} = \left\{ r + \left(\left\lfloor \frac{r}{2^j} \right\rfloor + 1 \right) 2^j \right\}_{r=0}^{M/2-1}$ denote, respectively, the subsets that contain all symbols whose labels have values 0 and 1 at the jth position. Furthermore, let $\alpha_j(\hat{s}) = \left(\frac{\hat{s}}{2^j} \mod 2 \right),\ j = 0, 1, \ldots, q-1,\ \hat{s} = 0, 1, \ldots, M-1$, which takes values from $0, 1$, as the jth bit associated with the symbol $\hat{s}$. Then the output distribution of the soft demapper is

related to the input distributions by Benedetto *et al.* [64] and be expressed as

$$\begin{aligned} p(b_{n,j}^{(k)}=1;O) &= \sum_{\hat{s}\in\mathcal{S}_j^{(1)}} P(s_n^{(k)}=\hat{s}) \prod_{\kappa=0,\kappa\neq j}^{q-1} p(x_{n,\kappa}^{(k)}=\alpha_\kappa(\hat{s});I) \\ &= \sum_{\hat{s}\in\mathcal{S}_j^{(1)}} P(s_n^{(k)}=\hat{s}) \prod_{\kappa=0,\kappa\neq j}^{q-1} \frac{\exp\left(\Lambda^I(x_{n,\kappa}^{(k)})\cdot\alpha_\kappa(\hat{s})\right)}{1+\exp\left(\Lambda^I(x_{n,\kappa}^{(k)})\right)}. \end{aligned} \tag{4.4}$$

Similarly,

$$p(b_{n,j}^{(k)}=0;O) = \sum_{\tilde{s}\in\mathcal{S}_j^{(0)}} P(s_n^{(k)}=\tilde{s}) \prod_{\kappa=0,\kappa\neq j}^{q-1} \frac{\exp\left(\Lambda^I(x_{n,\kappa}^{(k)})\cdot\alpha_\kappa(\tilde{s})\right)}{1+\exp\left(\Lambda^I(x_{n,\kappa}^{(k)})\right)}. \tag{4.5}$$

Substituting (4.4) and (4.5) into (4.3), the extrinsic LLR at the output of soft demapper can be found to be

$$\begin{aligned} \Lambda^O(b_{n,j}^{(k)}) &= \log\left(\frac{\sum_{\hat{s}\in\mathcal{S}_j^{(1)}} P(s_n^{(k)}=\hat{s}) \prod_{\kappa=0,\kappa\neq j}^{q-1} \frac{\exp\left(\Lambda^I(x_{n,\kappa}^{(k)})\cdot\alpha_\kappa(\hat{s})\right)}{1+\exp\left(\Lambda^I(x_{n,\kappa}^{(k)})\right)}}{\sum_{\tilde{s}\in\mathcal{S}_j^{(0)}} P(s_n^{(k)}=\tilde{s}) \prod_{\kappa=0,\kappa\neq j}^{q-1} \frac{\exp\left(\Lambda^I(x_{n,\kappa}^{(k)})\cdot\alpha_\kappa(\tilde{s})\right)}{1+\exp\left(\Lambda^I(x_{n,\kappa}^{(k)})\right)}}\right) \\ &= \log\left(\frac{\sum_{\hat{s}\in\mathcal{S}_j^{(1)}} P(s_n^{(k)}=\hat{s}) \prod_{\kappa=0,\kappa\neq j}^{q-1} \exp\left(\Lambda^I(x_{n,\kappa}^{(k)})\cdot\alpha_\kappa(\hat{s})\right)}{\sum_{\tilde{s}\in\mathcal{S}_j^{(0)}} P(s_n^{(k)}=\tilde{s}) \prod_{\kappa=0,\kappa\neq j}^{q-1} \exp\left(\Lambda^I(x_{n,\kappa}^{(k)})\cdot\alpha_\kappa(\tilde{s})\right)}\right) \\ &= \log\left(\sum_{\hat{s}\in\mathcal{S}_j^{(1)}} \exp\left(L(s_n^{(k)}=\hat{s}) + \sum_{\kappa=0,\kappa\neq j}^{q-1} \Lambda^I(x_{n,\kappa}^{(k)})\cdot\alpha_\kappa(\hat{s})\right)\right) \\ &\qquad - \log\left(\sum_{\tilde{s}\in\mathcal{S}_j^{(0)}} \exp\left(L(s_n^{(k)}=\tilde{s}) + \sum_{\kappa=0,\kappa\neq j}^{q-1} \Lambda^I(x_{n,\kappa}^{(k)})\cdot\alpha_\kappa(\tilde{s})\right)\right) \end{aligned} \tag{4.6}$$

Then after being de-interleaved, the output extrinsic LLR becomes the input *a priori* LLR $\Lambda^I(b_{n,i}^{(k)})$, which can be used as the soft input for the SISO decoder. It is pointed out that for the first iteration of the inner-loop, the extrinsic information is unknown, thus one sets $\Lambda^I(x_{n,j}^{(k)})=0$ and therefore (4.6) is equal to (3.24). This means that the soft demapper introduced in this chapter without the input of the extrinsic probabilistic information performs exactly the same as the bit LLR calculation block shown in Fig. 3.5.

Also note that the expression in 4.6 is often referred to as Log-MAP algorithm and can be simplified by applying approximations [65]. This is detailed in Appendix B.

4.3 Simulation Results and Discussion

This section provides the simulation results to verify the performance superiority of the improved receiver in terms of bits error rate (BER). Simulation parameters, if not specified, are the same with that of simulations at the end of Chapter 3. That is, all the transmitters employ constraint-length 7, rate-1/2 convolutional code. Signal processing method at the relay is PDAF and power consumption at the relay equals the sum of powers at all user nodes. First, shown in solid lines in Fig. 4.3 are the BER performance of the improved receiver with $M = 16$, $L = 4$, $K = 5$ and 5 inner-loop iterations. On the other hand, the dashed lines are the BERs measured after each stage of SIC iteration, where no inner-loop iteration is performed, which correspond to the performance of the receiver proposed in Chapter 3. It can be clearly seen that inner-loop iterations help improving the system's performance significantly. With 5 SIC iterations combined with 5 inner-loop iterations, the improved receiver delivers a gain of more than 2dB[1] (measured at the BER level of 10^{-4}). Surprisingly, by comparing the performance of the receiver in Chapter 3 at the *last* stage of SIC decoding against the performance of the improved receiver at the *first* stage of SIC decoding, one can clearly observe the advantage of inner-loop processing. Specifically, 5 inner-loop iterations yield better performance than 5 outer-loop iterations (by a remarkable 1dB[1]. Moreover, since each inner-loop iteration is less complex than one outer-loop iteration (because each inner-loop iteration does not involve any statistical calculation for multiuser interference cancellation), the overall computational complexity of the receiver is reduced.

Next, Fig. 4.4 shows the BER performance measured at the last stage of SIC decoding (i.e., after the 5th outer-loop) when different numbers of inner-loop iterations are executed (from 1 to 5). The largest performance improvement is realized when the SIC receiver moves from 1 to 2 inner-loop iterations. From the third inner-loop iteration, only marginal performance improvement is achieved with increasing number of inner-loop iterations. Considering the tradeoff between performance and complexity, it is suggested that only two or three inner-loop iterations should be executed per one SIC iteration.

[1]The 2dB and 1dB gains translate to 21% and 37% reduction in the transmitter power, respectively.

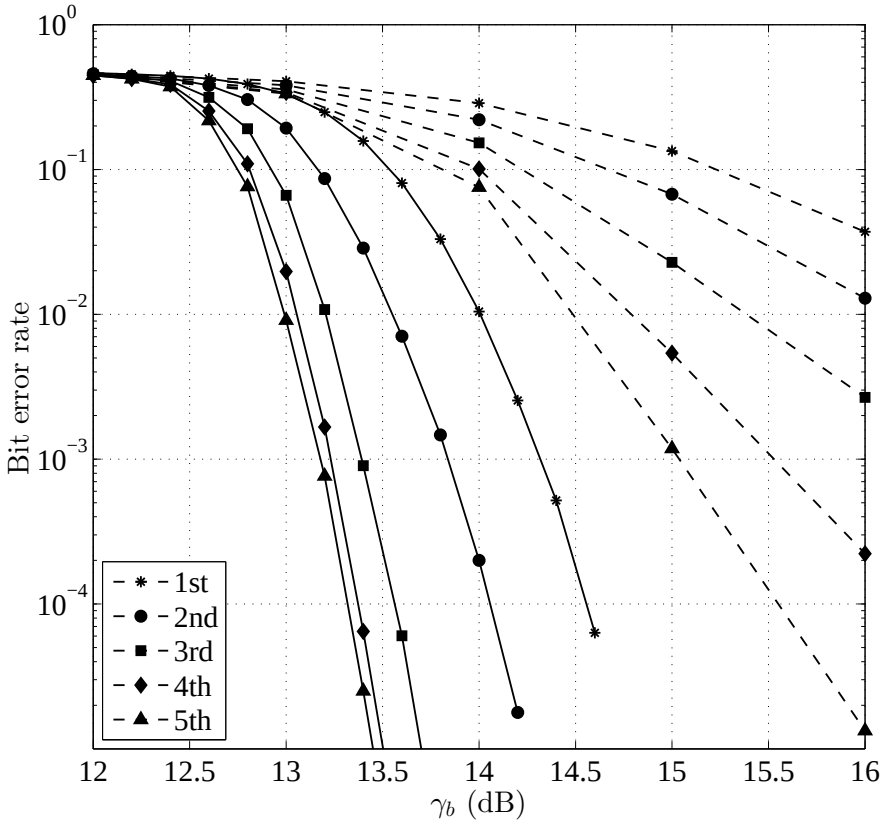

Figure 4.3 BER performance comparison between the improved receiver with $M = 16$ and 5 inner-loop iterations (solid lines) and the receiver in Chapter 3 without inner-loop (dashed lines).

Finally, to verify the effectiveness of the inner-loop operation, another set of simulation results with a different configuration is shown in Fig. 4.5. The purpose here is to show the performance evolution of the inner-loop iterations without the influence of the outer-loop. Therefore the system is configured with $M = 32$, $L = 5$ and $K = 1$. This means that there is only one user in the system and MAI does not exist nor there is a need to perform SIC (i.e., outer-loop iterations). The optimum convolutional code of rate-5/6 and constraint-length 7 [55] is selected and the simulation is limited to a maximum of 10 inner-loop iterations. Again, one can observe huge performance improvements with the first three inner-loop iterations.

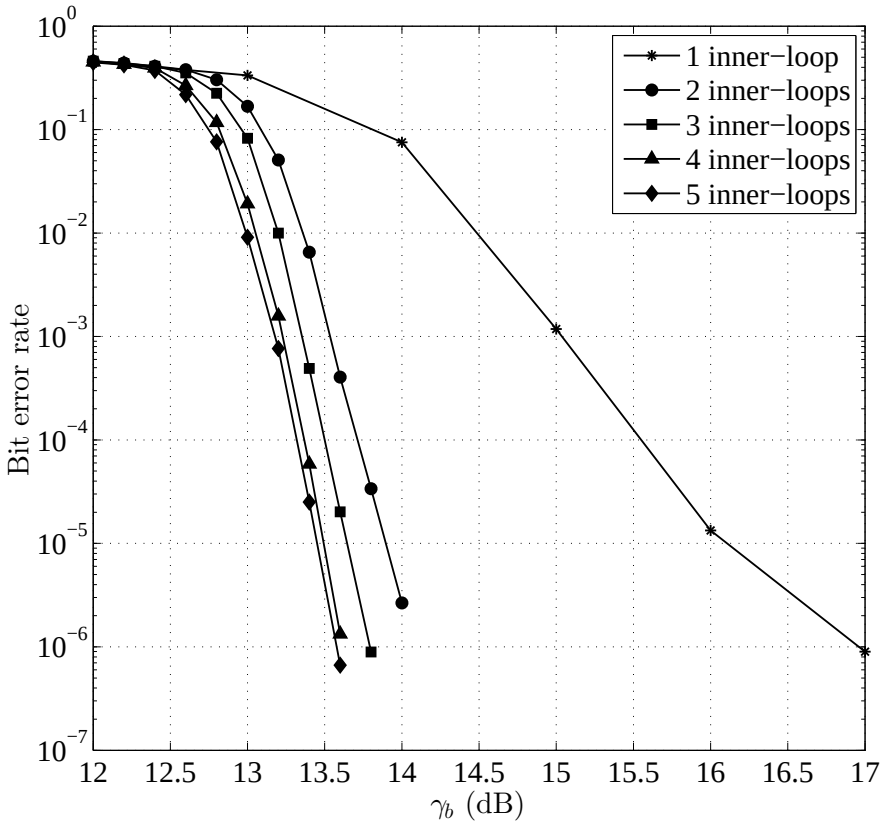

Figure 4.4 BER comparison for different numbers of inner-loop iterations.

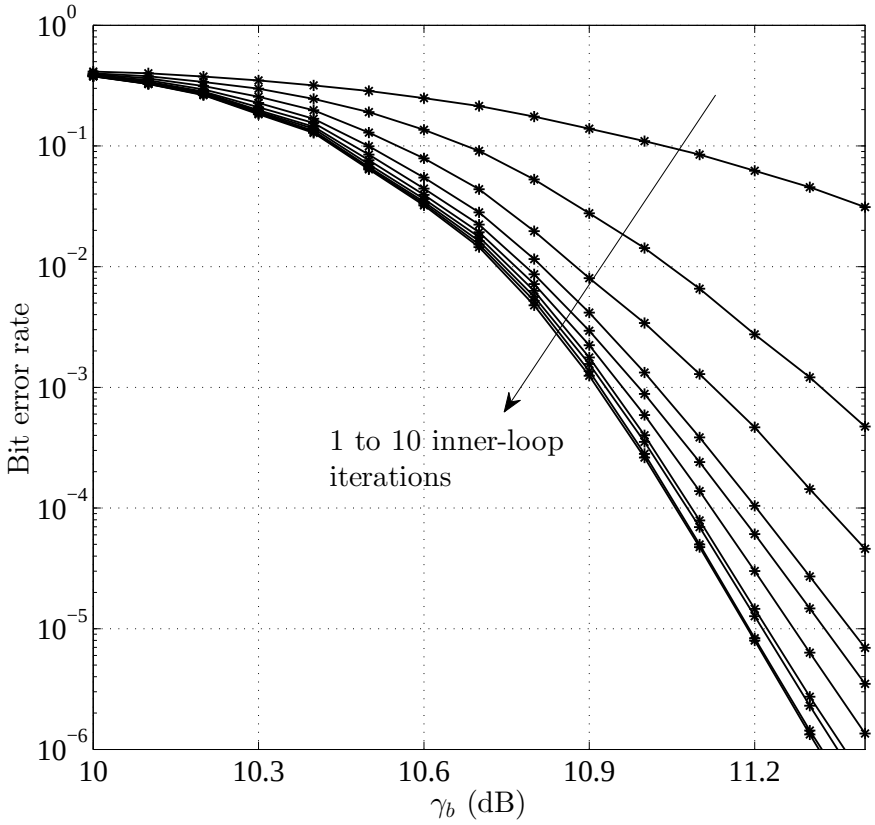

Figure 4.5 BER performance of single-user system with different numbers of inner-loop iterations.

5. Conclusions and Suggestions for Further Research

5.1 Conclusions

A novel iterative receiver has been developed for multi-user relaying communications in which each user employs fast frequency-hopping (FFH) modulation and channel coding, while the relay is either amplify-and-forward or partial decode-and-forward. To reduce the cost of implementation and increase communication reliability, an efficient method to mitigate multiuser interference is presented. In particular, an iterative signal processing scheme and related computations were devised to take advantage of the decoders' outputs for interference cancellation at the destination. Under flat Rayleigh fading channels, simulation results show impressive performance improvement of the proposed receiver with iterations. Under the same spectral efficiency and power consumption, the proposed system is shown to significantly outperform both the conventional coded and uncoded systems.

The iterative receiver is further improved with the introduction of inner-loop iterations. By properly exploiting the *extrinsic* information fed back from the SISO decoder, the receiver can incorporate several inner-loop iterations for every outer-loop iteration. It is pointed out that changing the numbers of inner loop and outer loop iterations is simple as it does not require to modify the receiver's hardware. In fact, the structure of the receiver is fixed and performing more iterations only increases the processing time and, as a consequence, introduces more latency. Simulation results indicate that a gain of 2dB can be attained with the improved implementation. It also shows that only two or three inner-loop iterations per each outer loop iteration should be executed to provide a reasonable trade off between performance and computational complexity.

While the framework is demonstrated for multiuser one-way relaying systems, the idea can be easily applied to the multi-way relaying systems by adopting the proposed iterative receiver at each user. In that case, each user only needs to recover the messages sent by other $(K-1)$ users. Another important point is that, although channel coding is used in the considered relaying systems, the complexity of the receiver is only linear in the number of users and frequency tones, whereas the complexity of the optimal ML-MUD is exponential in the numbers of users and frequency tones for the uncoded system. Therefore, the proposed receiver is much more attractive for implementation.

As modern hardware's processing speed increases exponentially over the years, the investigations in this thesis could potentially contribute to the development of next generations of broadcasting and communications systems. For example, since FFH modulation had been used to maintain connection among multiple Bluetooth® devices, the proposed interference cancellation technique might contribute to the development of the next generation of Bluetooth communications, which allows connectivity of more consumer devices with higher information throughput.

5.2 Suggestions for Further Research

This thesis proposes an iterative receiver and analyzes its performance in multiuser communications with two relaying schemes, namely the amplify-and-forward (AF) and partial decode-and-forward (PDAF). Although PDAF relaying gives better performance than the AF relaying, the choice of threshold used at the relay is sub-optimal. As such, finding an optimal threshold is an attractive subject for further research.

Also, in this thesis, the transmission is assumed to undergo flat Rayleigh fading. It is worth developing a detection framework for frequency-selective fading channels that are more common in broadband data transmission.

Although simulation with binary convolutional codes is made, the proposed algorithm should work for other types of codes as well, such as turbo or Low-Density Parity-Check (LDPC) codes. Determining an optimal selection of code type, code rate, number of chip

times and bandwidth to maximize the system throughput is an interesting problem. In this regard, the EXtrinsic Information Transfer (EXIT) chart could potentially be an useful tool.

A. Log-Domain Computations

One issue concerning the calculation of various expressions in Section 3.3.2 is the excessive growth of intermediate values. For example, the product of probabilities in (3.21) has the tendency of becoming zero or positive infinity in the cases of low and high signal-to-noise ratios, respectively. The situation is worse when M or L increases. A more reliable calculation is performed in the logarithm domain. First, define the following quantities, which are independent of the number of iterations at the receiver:

$$\begin{aligned} \xi_{n,m,l}^{[\nu]} &= \ln\left(P(T_{n,m,l}=0|s_n^{(k)}, U_{n,m,l}^{[\nu]})\right), && \text{(A.1)} \\ \zeta_{n,m,l}^{[\nu]} &= \ln\left(P\left(T_{n,m,l}=1|s_n^{(k)}, U_{n,m,l}^{[\nu]}\right)\right) \\ &= \ln\left(1-P\left(T_{n,m,l}=0|s_n^{(k)}, U_{n,m,l}^{[\nu]}\right)\right). && \text{(A.2)} \end{aligned}$$

Also define the log probability as $L(\cdot)=\ln(p(\cdot))$. Then (3.41) can be written as

$$\begin{aligned} L(Y_{n,m,l}|s_n^{(k)}, U_{n,m,l}^{[\nu]}) = \zeta_{n,m,l}^{[\nu]} - \frac{Y_{n,m,l}}{1+\sigma^2} - \ln(1+\sigma^2) + \\ \ln\left(1+\exp\left(\frac{-Y_{n,m,l}}{\sigma^2(1+\sigma^2)} + \ln(1+\sigma^2) - 2\ln(\sigma_n) + \xi_{n,m,l}^{[\nu]} - \zeta_{n,m,l}^{[\nu]}\right)\right), \quad \text{(A.3)} \end{aligned}$$

and

$$L(\mathbf{Y}_n|s_n^{(k)}, \mathbf{U}_n^{[\nu]}) = \sum_{m=0}^{M-1}\sum_{l=1}^{L} L(Y_{n,m,l}|s_n^{(k)}, U_{n,m,l}^{[\nu]}). \quad \text{(A.4)}$$

The symbol likelihood in (3.20) is given as

$$L(s_n^{(k)}|\mathbf{Y}_n, \mathbf{U}_n^{[\nu]}) = -\ln\left(1 + \sum_{\hat{s}=0,\hat{s}\neq s_n^{(k)}}^{M-1} \exp\left(L(\mathbf{Y}_n|\hat{s}, \mathbf{U}_n^{[\nu]}) - L(\mathbf{Y}_n|s_n^{(k)}, \mathbf{U}_n^{[\nu]})\right)\right). \quad \text{(A.5)}$$

It follows from (3.23) that the bit log likelihood values are

$$L(b_{n,j}^{(k)} = 0|\mathbf{Y}_n, \mathbf{U}_n^{[\nu]}) = \\ L(0|\mathbf{Y}_n, \mathbf{U}_n^{[\nu]}) + \ln\left(1 + \sum_{r=1}^{(M/2)-1} \exp\left(L(\hat{s}|\mathbf{Y}_n, \mathbf{U}_n^{[\nu]}) - L(0|\mathbf{Y}_n, \mathbf{U}_n^{[\nu]})\right)\right), \quad \text{(A.6)}$$

where $\hat{s} = r + \left\lfloor \frac{r}{2^j} \right\rfloor \cdot 2^j$. Finally, the log-likelihood ratio in (3.24) can be written as

$$\Lambda(b_{n,j}^{(k)}) = \ln\left(1 - \exp\left(L(b_{n,j}^{(k)} = 0|\mathbf{Y}_n, \mathbf{U}_n^{[\nu]})\right)\right) - L(b_{n,j}^{(k)} = 0|\mathbf{Y}_n, \mathbf{U}_n^{[\nu]}). \quad \text{(A.7)}$$

B. Sub-Optimal Log-MAP Algorithms

In Section 4.2, an expression to calculate the soft demapper's extrinsic likelihood ratios was given. The equation, in its original form, is difficult to implement because of the numerical representation of probabilities and non-linear operations such as exponentiation and multiplication. In fact, the demand for high data throughput requires a very fast calculation of these functions. Using software algorithms to generate these elementary functions is often not fast enough [66], therefore, the use of dedicated hardware to compute multiplication (while exponentiation module can be made from several multiplications [66]) is of great value. As a consequence, in modern DSP implementations, the cost of devices is strongly influenced by a number of embedded multiplication components. Fortunately, by performing the computation in the log domain, the complexity is significantly reduced because multiplications can be replaced by addition operations. However there is still a technical difficulty in taking logarithm of the summation in (4.6). Several sub-optimal methods that can avoid such computation difficulty are presented in the following sections.

B.1 Max-Log-MAP Algorithm

It is pointed out that the summation of multiple exponential functions is dominated by the function with the largest argument. Therefore, for a finite set of real numbers $\{\lambda_i\}$, $i = 1, \ldots, n$, one can make use of the following approximation:

$$\log\big(\exp(\lambda_1) + \exp(\lambda_2) + \ldots + \exp(\lambda_n)\big) \approx \max_{i\in\{1,\ldots,n\}} \{\lambda_i\}, \tag{B.1}$$

When using the above approximation, the MAP algorithm becomes the Max-Log-MAP algorithm [65]. Specifically, (4.6) becomes

$$\Lambda^O(b_{n,j}^{(k)}) = \max_{\hat{s}\in\mathcal{S}_j^{(1)}} \left\{ L(s_n^{(k)} = \hat{s}) + \sum_{\kappa=0,\kappa\neq j}^{q-1} \Lambda^I(x_{n,\kappa}^{(k)}) \cdot \alpha_\kappa(\hat{s}) \right\} - \max_{\tilde{s}\in\mathcal{S}_j^{(0)}} \left\{ L(s_n^{(k)} = \tilde{s}) + \sum_{\kappa=0,\kappa\neq j}^{q-1} \Lambda^I(x_{n,\kappa}^{(k)}) \cdot \alpha_\kappa(\tilde{s}) \right\}. \quad \text{(B.2)}$$

B.2 Max-Star Algorithm

Because of the approximation in (B.1), the Max-Log-MAP algorithm is clearly sub-optimal and yields inferior soft outputs when compared to the original log-MAP algorithm. To exactly calculate $\log\left(\sum_{i=1}^{n}\exp(\lambda_i)\right)$, Viterbi introduced a *max-star* function [67], which can be defined recursively from a pair-wise operator:

$$\begin{aligned} \max^*(\lambda_1,\lambda_2) \equiv \log(\exp(\lambda_1)+\exp(\lambda_2)) &= \max\{\lambda_1,\lambda_2\} + \log(1+\exp(-|\lambda_1-\lambda_2|)) \\ &= \max\{\lambda_1,\lambda_2\} + f_c(|\lambda_1-\lambda_2|), \end{aligned} \quad \text{(B.3)}$$

where $f_c(|\lambda_1-\lambda_2|)$ is a correction function for the conventional Max-Log-MAP algorithm. When deriving the max-star algorithm, all maximizations over two values are augmented with the correction function. As a consequence, by correcting, at each step, the approximation made by the Max-Log-MAP, one can preserve the original log-MAP algorithm. The max-star function can be defined for multiple arguments by recursively applying the pair-wise operation. That is

$$\begin{aligned} \max^*(\lambda_1,\lambda_2,\lambda_3) &= \max^*\left(\max^*(\lambda_1,\lambda_2),\lambda_3\right) \\ &= \log(\exp(\lambda_1)+\exp(\lambda_2)+\exp(\lambda_3)), \end{aligned} \quad \text{(B.4)}$$

and so on.

For the expression in (B.3), note that the $\max\{\cdot\}$ function is simple to implement in hardware as it only consists of simple bit comparators. Moreover, since the correction function $f_c(\cdot)$ only depends on $|\lambda_1-\lambda_2|$, is only needs *one* dimensional lookup table to generate an output based on *two* input arguments. Therefore, the max-star algorithm's complexity is significantly lower than that of the log-MAP algorithm. However, calculating $f_c(|\lambda_1-\lambda_2|)$

introduces complexity of its own. Fortunately, Roberson *et al.* [65] pointed out that excellent approximation can be attained by using a correction table that stores only 8 values of $f_c(\cdot)$, which are associated with the input arguments $\{|\lambda_1 - \lambda_2|\}$ ranging from 0 to 5. Using the suggested 8-entries correction table for the max-star algorithm, the expression in (4.6) can be approximated as follows:

$$\Lambda^O(b_{n,j}^{(k)}) = \max_{\hat{s}\in\mathcal{S}_j^{(1)}}{}^{*} \left\{ L(s_n^{(k)} = \hat{s}) + \sum_{\kappa=0,\kappa\neq j}^{q-1} \Lambda^I(x_{n,\kappa}^{(k)}) \cdot \alpha_\kappa(\hat{s}) \right\} - \max_{\tilde{s}\in\mathcal{S}_j^{(0)}}{}^{*} \left\{ L(s_n^{(k)} = \tilde{s}) + \sum_{\kappa=0,\kappa\neq j}^{q-1} \Lambda^I(x_{n,\kappa}^{(k)}) \cdot \alpha_\kappa(\tilde{s}) \right\}. \quad \text{(B.5)}$$

References

[1] A. Goldsmith, *Wireless Communications*. New York, NY, USA: Cambridge University Press, 2005.

[2] J. M. Shea, "History of Wireless Communication." `http://wireless.ece.ufl.edu/jshea/HistoryOfWirelessCommunication.html`, Dec. 2011. [Sep. 1,2013].

[3] Wikipedia, "Telegraphy." `http://en.wikipedia.org/wiki/Telegraph`, Aug. 2013. [Sep. 1,2013].

[4] P. P. Munoz, "Wireless Telecommunication Industry Overview." `http://www.columbia.edu/cu/consultingclub/Resources/Telecommunications_Pablo_PrietoMunoz.pdf`, Feb. 2012. [Sep. 1,2013].

[5] B. Sanou, "The World in 2013: ICT Facts and Figures," *Int. Telegraph Union*, Feb. 2013.

[6] D. Gesbert, M. Shafi, D. shan Shiu, P. Smith, and A. Naguib, "From theory to practice: an overview of MIMO space-time coded wireless systems," *IEEE J. Select. Areas in Commun.*, vol. 21, pp. 281–302, Mar. 2003.

[7] G. N. Thayer, A. A. Roetken, R. W. Friis, and A. L. Durkee, "A broad-band microwave relay system between New York and Boston," *Proc. of the IRE*, vol. 37, pp. 183–188, Feb. 1949.

[8] S. P. Brown, "Project SCORE: Signal Communication by Orbiting Relay Equipment," *IRE Trans. on Military Electronics*, vol. 4, pp. 193–194, July 1960.

[9] T. Kasami and S. Lin, "Coding for a multiple-access channel," *IEEE Trans. Inform. Theory*, vol. 22, pp. 129–137, Mar. 1976.

[10] H. Liao, "A coding theorem for multiple access communications," in *Proc. IEEE Int. Symp. Inform. Theory*, Jan. 1972.

[11] T. M. Cover, "Some advances in broadcast channels," *New York:Academic Press Advances in Commun. Systems*, vol. 4, pp. 229–260, July 1975.

[12] A. Wyner, "Recent results in the Shannon theory," *IEEE Trans. Inform. Theory*, vol. 20, pp. 2–10, Jan. 1974.

[13] S.-C. Chang and E. Weldon, "Coding for T-user multiple-access channels," *IEEE Trans. Inform. Theory*, vol. 25, pp. 684–691, Nov. 1979.

[14] T. Kasami and S. Lin, "Coding for a multiple-access channel," *IEEE Trans. Inform. Theory*, vol. 22, pp. 129–137, Mar. 1976.

[15] T. Kasami and S. Lin, "Bounds on the achievable rates of block coding for a memoryless multiple-access channel," *IEEE Trans. Inform. Theory*, vol. 24, pp. 187–197, Mar. 1978.

[16] H. van Tilborg, "An upper bound for codes in a two-access binary erasure channel (Corresp.)," *IEEE Trans. Inform. Theory*, vol. 24, pp. 112–116, Jan. 1978.

[17] C. Berrou, A. Glavieux, and P. Thitimajshima, "Near Shannon limit error-correcting coding and decoding: Turbo-codes. 1," in *Proc. IEEE Int. Conf. Commun.*, vol. 2, pp. 1064–1070 vol.2, May 1993.

[18] C. Berrou and A. Glavieux, "Near optimum error correcting coding and decoding: turbo-codes," *IEEE Trans. Commun.*, vol. 44, pp. 1261–1271, Oct. 1996.

[19] M. Moher, "An iterative multiuser decoder for near-capacity communications," *IEEE Trans. Commun.*, vol. 46, pp. 870–880, July 1998.

[20] M. Reed, C. Schlegel, P. Alexander, and J. Asenstorfer, "Iterative multiuser detection for CDMA with FEC: near-single-user performance," *IEEE Trans. Commun.*, vol. 46, pp. 1693–1699, Dec. 1998.

[21] X. Wang and H. Poor, "Iterative (turbo) soft interference cancellation and decoding for coded CDMA," *IEEE Trans. Commun.*, vol. 47, pp. 1046–1061, July 1999.

[22] L. Ping, L. Liu, and W. K. Leung, "A simple approach to near-optimal multiuser detection: interleave-division multiple-access," in *Proc. IEEE Wireless Commun. and Networking. Conf.*, vol. 1, pp. 391–396, Mar. 2003.

[23] L. Ping, L. Liu, K. Y. Wu, and W. K. Leung, "Approaching the capacity of multiple access channels using interleaved low-rate codes," *IEEE Commun. Letters*, vol. 8, pp. 4–6, Jan. 2004.

[24] C. Waylan, "Detection of fast, noncoherent, frequency-hopped FSK," *IEEE Trans. Commun.*, vol. 23, pp. 543–546, May 1975.

[25] R. Kozick and B. Sadler, "Maximum likelihood multi-user detection for fast frequency hopping/multiple frequency shift keying systems," in *Proc. IEEE Wireless Commun. and Networking. Conf.*, vol. 1, pp. 67–72, Sept. 2000.

[26] X. Wang and H. V. Poor, *Wireless communication systems: advanced techniques for signal reception.* Prentice Hall PTR, 1st ed., Sept. 2003.

[27] A. Nosratinia, T. Hunter, and A. Hedayat, "Cooperative communication in wireless networks," *IEEE Commun. Mag.*, vol. 42, pp. 74–80, Oct. 2004.

[28] P. Anghel and M. Kaveh, "Exact symbol error probability of a Cooperative network in a Rayleigh-fading environment," *IEEE Trans. on Wireless Commun.*, vol. 3, pp. 1416–1421, Oct. 2004.

[29] J. Cao, L.-L. Yang, and Z. Zhong, "Noncoherent multi-way relay based on fast frequency-hopping M-ary frequency-shift keying," in *Proc. IEEE Int. Symp. on Wireless Commun. Systems*, pp. 250 –254, Sept. 2010.

[30] L. Ong, S. Johnson, and C. Kellett, "An optimal coding strategy for the binary multi-way relay channel," *IEEE Commun. Letters*, vol. 14, pp. 330–332, Apr. 2010.

[31] D. Gunduz, A. Yener, A. Goldsmith, and H. Poor, "The Multiway Relay Channel," *IEEE Trans. Inform. Theory*, vol. 59, pp. 51–63, Jan. 2013.

[32] G. Kramer, M. Gastpar, and P. Gupta, "Cooperative strategies and capacity theorems for relay networks," *IEEE Trans. Inform. Theory*, vol. 51, pp. 3037–3063, Sept. 2005.

[33] M. Souryal and B. Vojcic, "Performance of Amplify-and-Forward and Decode-and-Forward relaying in Rayleigh fading with Turbo Codes," in *Proc. IEEE Int. Conf. on Acoustics, Speech, and Signal Processing*, vol. 4, pp. IV–IV, May 2006.

[34] D. Tse and P. Viswanath, *Fundamentals of Wireless Communication*. Cambridge University Press, July 2005.

[35] European Telecommunications Standards Institute (ETSI), "GSM Technical Specification," Apr. 1998.

[36] G. Cooper and R. Nettleton, "A spread-spectrum technique for high-capacity mobile communications," *IEEE Trans. Veh. Technol.*, vol. 27, pp. 264–275, Nov. 1978.

[37] A. J. Viterbi, "A processing satellite transponder for multiple access by low-rate mobile users," in *Int. Conf. on Digital Satellite Commun.*, pp. 166–174, 1979.

[38] G. Einarsson, "Adddress assignment for a time-frequency-coded, spread spectrum systems," *Bell System Tech. J.*, vol. 59, pp. 1241–1255, Sept. 1980.

[39] B. Haskell, "Computer simulation results on fequency hopped MFSK mobile radio-noiseless case," *IEEE Trans. Commun.*, vol. 29, pp. 125–132, Feb. 1981.

[40] D. J. Goodman, P. S. Henry, and V. K. Prabhu, "Frequency-hopped multilevel FSK for mobile radio," *Bell System Tech. J.*, vol. 59, pp. 1257–1275, Sept. 1980.

[41] T. Mabuchi, R. Kohno, and H. Imai, "Multiuser detection scheme based on canceling cochannel interference for MFSK/FH-SSMA system," *IEEE J. Select. Areas in Commun.*, vol. 12, pp. 593–604, May 1994.

[42] U.-C. Fiebig, "Iterative interference cancellation for FFH/MFSK MA systems," *Proc. IEEE Int. Conf. Commun.*, vol. 143, pp. 380–388, Dec. 1996.

[43] U.-C. Fiebig and P. Robertson, "Soft-decision and erasure decoding in fast frequency-hopping systems with convolutional, turbo, and Reed-Solomon codes," *IEEE Trans. Commun.*, vol. 47, pp. 1646–1654, Nov. 1999.

[44] D. Park and B. G. Lee, "Iterative decoding in convolutional and turbo coded MFSK/FH-SSMA systems," in *Proc. IEEE Int. Conf. Commun.*, vol. 9, pp. 2784–2788 vol.9, 2001.

[45] O.-C. Yue, "Maximum likelihood combining for noncoherent and differentially coherent Frequency-Hopping Multiple-Access systems," *IEEE Trans. Inform. Theory*, vol. 28, pp. 631–639, July 1982.

[46] S. Ahmed, R. Maunder, L.-L. Yang, S. X. Ng, and L. Hanzo, "Joint Source Coding, Unity Rate Precoding and FFH-MFSK Modulation Using Iteratively Decoded Irregular Variable Length Coding," in *Proc. IEEE Veh. Technol. Conf.*, pp. 1042–1046, Oct. 2007.

[47] S. Ahmed, S. X. Ng, L.-L. Yang, and L. Hanzo, "Iterative Decoding and Soft Interference Cancellation in Fast Frequency Hopping Multiuser System Using Clipped Combining," in *Proc. IEEE Wireless Commun. and Networking. Conf.*, pp. 723–728, Mar. 2007.

[48] S. Ahmed, L.-L. Yang, L. Hanzo, and F. Guo, "Soft Decoding Assisted Interference Cancellation in a Non-Binary LDPC Coded Fast Frequency Hopping Multiuser System Using Product Combining," in *Proc. IEEE Veh. Technol. Conf.*, pp. 1717–1721, Oct. 2007.

[49] C. Hung and Y. Su, "Diversity combining considerations for incoherent frequency hopping multiple access systems," *IEEE J. Select. Areas in Commun.*, vol. 13, pp. 333–344, Feb. 1995.

[50] S.-H. Lee and Y.-H. Lee, "Adaptive frequency hopping for bluetooth robust to WLAN interference," *IEEE Commun. Letters*, vol. 13, pp. 628–630, Sept. 2009.

[51] K. Halford and M. Brandt-Pearce, "Multistage multiuser detection for FHMA," *IEEE Trans. Commun.*, vol. 48, pp. 1550–1562, Sept. 2000.

[52] Y.-S. Liu, "Diversity-combining and error-correction coding for FFH/MFSK Systems over Rayleigh fading channels under multitone jamming," *IEEE Trans. on Wireless Commun.*, vol. 11, pp. 771–779, Feb. 2012.

[53] Y. Zhu, P.-Y. Kam, and Y. Xin, "Non-coherent detection for Amplify-and-Forward relay systems in a Rayleigh fading environment," in *Proc. IEEE Global Telecommun. Conf.*, pp. 1658–1662, Nov. 2007.

[54] S. Lin and D. Costello, *Error control coding: fundamentals and applications.* Prentice-Hall computer applications in electrical engineering series, Prentice-Hall, 2 ed., May 2004.

[55] H. Sasano and S. Moriya, "A construction of high rate punctured convolutional codes," in *Proc. IEEE Int. Symp. Inform. Theory and Its Appl.*, pp. 662–666, Oct. 2012.

[56] E. Zehavi, "8-PSK trellis codes for a Rayleigh channel," *IEEE Trans. Commun.*, vol. 40, pp. 873–884, May 1992.

[57] G. Caire, G. Taricco, and E. Biglieri, "Bit-interleaved coded modulation," *IEEE Trans. Inform. Theory*, vol. 44, pp. 927–946, May 1998.

[58] G. Ungerboeck, "Channel coding with multilevel/phase signals," *IEEE Trans. Inform. Theory*, vol. 28, pp. 55–67, Jan. 1982.

[59] S. Ten Brink, J. Speidel, and R.-H. Yan, "Iterative demapping and decoding for multi-level modulation," in *Proc. IEEE Global Telecommun. Conf.*, vol. 1, pp. 579–584 vol.1, Nov. 1998.

[60] N. H. Tran, *Exploiting Diversity In Wireless Channels With Bit-Interleaved Coded Modulation And Iterative Decoding (BICM-ID).* PhD thesis, University of Saskatchewan, Dec. 2007.

[61] P. Hoeher and J. Lodge, " "Turbo DPSK" : iterative differential PSK demodulation and channel decoding," *IEEE Trans. Commun.*, vol. 47, pp. 837–843, June 1999.

[62] J. Forney, G.D., "The Viterbi algorithm," *Proc. IEEE*, vol. 61, pp. 268–278, Mar. 1973.

[63] L. Bahl, J. Cocke, F. Jelinek, and J. Raviv, "Optimal decoding of linear codes for minimizing symbol error rate," *IEEE Trans. Inform. Theory*, vol. 20, pp. 284–287, Mar. 1974.

[64] S. Benedetto, D. Divsalar, G. Montorsi, and F. Pollara, "Soft-Input Soft-Output modules for the construction and distributed iterative decoding of code networks," *Eur. Trans. on Telecommun.*, vol. 9, pp. 155–172, Mar.-Apr. 1998.

[65] P. Robertson, E. Villebrun, and P. Hoeher, "A comparison of optimal and sub-optimal MAP decoding algorithms operating in the log domain," in *Proc. IEEE Int. Conf. Commun.*, vol. 2, pp. 1009–1013 vol.2, June 1995.

[66] J.-A. Pineiro, M. Ercegovac, and J. Bruguera, "Algorithm and architecture for logarithm, exponential, and powering computation," *IEEE Trans. on Comp.*, vol. 53, pp. 1085–1096, Sept. 2004.

[67] A. Viterbi, "An intuitive justification and a simplified implementation of the MAP decoder for convolutional codes," *IEEE J. Select. Areas in Commun.*, vol. 16, pp. 260–264, Feb. 1998.